INFORMATION TO USERS

This manuscript has been reproduced from the microfilm master. UMI films the text directly from the original or copy submitted. Thus, some thesis and dissertation copies are in typewriter face, while others may be from any type of computer printer.

The quality of this reproduction is dependent upon the quality of the copy submitted. Broken or indistinct print, colored or poor quality illustrations and photographs, print bleedthrough, substandard margins, and improper alignment can adversely affect reproduction.

In the unlikely event that the author did not send UMI a complete manuscript and there are missing pages, these will be noted. Also, if unauthorized copyright material had to be removed, a note will indicate the deletion.

Oversize materials (e.g., maps, drawings, charts) are reproduced by sectioning the original, beginning at the upper left-hand corner and continuing from left to right in equal sections with small overlaps. Each original is also photographed in one exposure and is included in reduced form at the back of the book.

Photographs included in the original manuscript have been reproduced xerographically in this copy. Higher quality 6" x 9" black and white photographic prints are available for any photographs or illustrations appearing in this copy for an additional charge. Contact UMI directly to order.

UMI®

Bell & Howell Information and Learning
300 North Zeeb Road, Ann Arbor, MI 48106-1346 USA
800-521-0600

Characterization of Surfactant Adsorption at a Liquid-Liquid Interface by Drop Volume Tensiometry

Xiaohong Wang

A Thesis

in

The School

for

Building

(Civil Engineering Program)

Presented in Partial Fulfillment of the Requirements
for the Degree of Master of Applied Science at

Concordia University

Montreal, Quebec, Canada

July 1997

ABSTRACT

Characterization of Surfactant Adsorption at a Liquid-Liquid Interface by Drop Volume Tensiometry

by Xiaohong Wang

Surfactant characterization is important for many practical applications, such as the removal of hydrophobic contaminants from soils through surfactant-enhanced washing or flushing processes. Dynamic interfacial tension measurements can be useful in describing the adsorption behavior of surfactants at liquid-liquid interfaces. In this work, selected surfactants are tested at the mineral oil-water interface using a drop volume tensiometer. A model is developed to account for the neck formation in suspended drops under certain experimental conditions. The model relates apparent values of interfacial tension calculated from drops possessing necks to actual values. Dynamic interfacial tension measurements are then used to describe surfactant adsorption.

In many cases, surfactant adsorption can be described by either kinetic or diffusion-controlled models. A kinetic-controlled model is found to fit the dynamic interfacial tension data obtained for sodium dodecyl sulfate. Span 80 and Triton X-100 are found to

fit diffusion-controlled models. For Span 80 dissolved in the mineral oil phase, the short diffusion time approximation is valid. For Triton X-100 dissolved in the aqueous phase, the long diffusion time approximation is valid. A dimensionless parameter relating adsorption time, t_a, to a characteristic diffusion time, τ_D, is introduced in order to determine the general applicability of the diffusion approximations. The ratio t_a/τ_D is found to be useful in characterizing diffusion-controlled adsorption.

Acknowledgments

I would like to thank Dr. J. R. Campanelli for his knowledgeable input and guidance throughout the duration of this research.

I would like to also acknowledge:

- Mr. Ron Parisella for his aid in the photographic work.
- My parents and husband for their great support.
- The Faculty Research Development Program of Concordia and FCAR for their support of this research.

Table of Contents

List of Figures

List of Tables

Chapter 1. Introduction

Chemical releases into soils are pervasive environmental problems. Soil contaminants, such as hydrophobic organic compounds (HOCs) and heavy metal ions, can be typically found near some pipelines, gasoline stations, chemical plants and other facilities. These contaminants can migrate into the water table posing significant risks to the biosphere. Humans are exposed to these risks through their consumption of contaminated plants, animals, and water. Remediation of contaminated soil is thus a human health issue, as well as an environmental subject. However, remediation of releases of contaminants is a formidable challenge because the efforts are frequently inhibited by an inability to extract contaminants from the soil due to the significant sorption of strongly hydrophobic chemicals, or due to the presence of multiple liquid phases. Nevertheless, several technologies have been explored in order to clean up contaminated sites. Some of the more popular techniques include pump-and-treat, surfactant-enhanced remediation, and bioremediation. (Borchardt, 1995). Significant problems need to be overcome in order to maximize the efficiency of these processes.

Releases of organic compounds represent a major source of soil pollution. As the non-aqueous phase liquid (NAPL) is transported through the soil, a portion of the organic phase will be retained within soil pores as immobile ganglia or globules due to interfacial forces. This entrapped NAPL may occupy between 5 to 40 % of the total pore volume (Pennell *et al.*, 1993). Due to the low solubility of many NAPLs, the residual organic

phase frequently represents a long-term source of groundwater contamination. In addition, the concentration of NAPLs in groundwater rarely exceeds 10 % of their aqueous solubility. This phenomenon has been attributed to irregular NAPL distributions, non-uniform flow patterns, and dilution effects, as well as rate-limited mass transfer between the organic and aqueous phases (Nash, 1987). These low concentration NAPLs are extremely difficult to remove.

Surfactant-enhanced remediation has been proposed as an important method for recovery of residual NAPLs from contaminated aquifers. This technology is based primarily on two processes: increasing the solubility of HOCs in the aqueous phase, or enhancing the mobilization of HOCs (Pennell *et al.*, 1996). Surfactants are amphiphilic compounds that possess both hydrophilic and lipophilic moieties. The surfactant molecules that are present in one bulk phase will be transported from the bulk phase to the interface due to the concentration gradient and to their amphiphilic nature. At the interface, surfactants lower the interfacial forces that act to retain the HOCs.

Surfactants can also form micelles in the bulk phase. A micelle is an aggregate consisting of surfactant molecules oriented in a very specific manner with the hydrophobic moiety, or tail, facing inward and the hydrophilic head facing outward. Such a configuration minimizes the free energy of the water / surfactant system. The HOC molecules can enter the hydrophobic interior of the micelle and become solubilized within the micelle so that the aqueous phase solubility of the HOCs in increased. There is a critical micelle concentration (cmc), below which surfactants exist primarily as monomers. Below the

cmc, surfactants have a minimal effect on the solubility of most HOCs. Above the cmc, a dramatic enhancement in HOC solubility is commonly observed. Any micelle-forming surfactant is capable of solubilizing HOCs.

The process of mobilization is based on the *in-situ* formation of HOC-water emulsions through the lowering of interfacial tension. Surfactants which produce ultralow interfacial tension ($< 10^{-3}$ mN/m) between the organic and aqueous phase tend to form microemulsions (Sabatini *et al.*, 1995). Microemulsions allow the displacement or mobilization of residual NAPLs from porous media under normal flow regimes. In theory, this approach could offer an efficient means of recovering NAPLs from contaminated aquifers. However, some important theoretical concepts are still uncertain in employing such systems for aquifer remediation. For example, the parameters which affect the formation and stability of microemulsions are not fully understood for even the simplest systems.

The use of low concentrations of surfactants may also lead to the formation and transport of NAPL in water macroemulsion. A macroemulsion contains disperse phase droplets having diameters greater than 1 μm, and are not as stable as microemulsions. The formation and transport of macroemulsions are important for a variety of reasons (Okuda *et al.*, 1996). Surfactants that are good solubilizers also tend to form macroemulsions. Macroemulsions likely affect the aqueous-phase permeability of porous media. Macroemulsions may be mobile, so controlling their movement during surfactant flushing

in the soil is essential. Finally, solubilization kinetics may be affected by macroemulsification. Despite their importance in soil remediation, the *in-situ* formation of macroemulsions has not been considered explicitly in the past, and their transport in porous media has received little attention (Kokal, 1992).

Recent studies have reported the successful use of aqueous surfactant solutions to remove sorbed or deposited polychlorinated biphenyls (PCBs) and polycyclic aromatic hydrocarbons (PAHs) from soil materials (Mackay and Cherry, 1989; Wilson *et al.*, 1990). However, the recovery of free and residual hydrocarbons has proven to be far more difficult. Okuda *et al.* (1996) observed and quantified the removal of residual tetrachloroethylene (PCE) by a number of processes including dissolution, micellar emulsion / microemulsion transport, and macroemulsion transport, as a function of surfactant concentration used to elute the PCE from the porous medium. They concluded that macroemulsion transport was an important process, accounting for up to 30 % of total PCE removal. Fountain *et al.* (1991) also identified a number of surfactant formulations capable of removing PCE from soil columns after injecting 7 to 14 pore volumes of surfactant solution. The mixed results of the surfactant remediation studies conducted to date emphasize the need for fundamental research on the processes governing surfactant-enhanced aquifer remediation.

One conclusion of past mobilization studies is that in order to induce NAPL mobilization, the reduction in interfacial tension (γ) between the aqueous and organic phases must be

sufficient to overcome the capillary forces acting to retain the organic liquids within a porous medium. Thus, interfacial tension is one of the most important parameters in surfactant-enhanced remediation. The Capillary number (N_{Ca}) and Bond number (N_B) are dimensionless groups that have been employed to assess the impact of viscous and buoyancy forces on the mobilization of NAPLs in porous media (Weber and Digiano, 1996). These expressions can be defined as follows:

$$N_{ca} = \mu_w \, q \, / \, \gamma_{ow} \qquad [1.1]$$

$$N_B = \Delta\varrho \, g \, d_p^{\,2} \, / \, \gamma_{ow} \qquad [1.2]$$

where γ_{ow} is the interfacial tension between the organic and aqueous phases; μ_w is the viscosity of water; q is the Darcy velocity; d_p is the diameter of a particle in the porous media; and $\Delta\varrho$ is the difference in fluid densities.

Interfacial tension appears explicitly in both Equations [1.1] and [1.2]. Interfacial tension is the work required to cause a unit increase in interfacial area at equilibrium. However, when an impurity such as a surfactant is present at the interface, the interfacial tension will decrease, and becomes time dependent. This transient nature of γ is referred to as dynamic interfacial tension. Since the mobilization of NAPLs in soil results in continuous formation of interfacial area, dynamic interfacial tension can be expected to play a more important role than the equilibrium interfacial tension. Adeel and Luthy (1995) have recently noted the difficulties encountered when dynamic values of γ are neglected. In this work, dynamic interfacial tension is measured for various surfactants at the water-

HOC interface. The experimental data are used to model the surfactant adsorption, and to elucidate the adsorption mechanisms. The results may be useful for studies of NAPL mobilization processes in porous media.

Chapter 2. Literature Review

2.1 Surface and Interfacial Tension

The concept of surface tension dates back to the early ideas that the surface of a liquid possesses some kind of contractile "skin". The thermodynamic definition of surface tension is the work required to increase the area of a surface per unit surface area (Adamson, 1990). Although defined as a free energy per unit area, surface tension may also be thought of as a force per unit length, and is frequently expressed in the S. I. units mN/m.

The same basic ideas that are used to describe the liquid-vapor interface apply to the liquid-liquid interface. When both of the immiscible phases are liquids, the term interfacial tension replaces surface tension. Since a second liquid phase is much more dense than a vapor phase, the various attractive interactions among molecules in each phase across the interface are significantly greater. As a result, for a given increase in interfacial area, the excess energy at a liquid-liquid interface will be lower. In other words, the net work required to increase the interfacial area, the interfacial tension, will be reduced relative to the surface tension. This fact leads to two general conclusions (Myers, 1991). First of all, the interfacial tension between a given liquid and water is always less than the surface tension of water. Secondly, for an homologous series of materials such as the normal alkanes, the interfacial tension between the members of the

series and water will change only slightly as a function of the molecular weight of the material. These two characteristics are a direct consequence of the nature of the interactions at the interface. Where the two liquids are highly immiscible, the interfacial tension will lie between the two surface tensions. If significant miscibility exists, the interfacial tension will be lower than the lower of the two surface tensions.

As mentioned before, dynamic interfacial tension is more important than the equilibrium value in soil washing and flushing applications due to the continuous formation of HOC-water interface. The typical dynamic surface tension versus log time curve is divided into four regions: an induction region, a fast fall region, a plateau region, and finally an equilibrium region. Hua and Rosen (1988) studied the dynamic surface tension of sodium di(2-ethylhexyl) sulfosuccinate (DESS) solution and n-dodecyl-n-benzyl-n-methylglycine (C_{12}-BMG) solution. They demonstrated that the first three regions are more important in dynamic processes. Figure 2.1 represents a generalized dynamic surface tension versus log time curve for the first three regions. In the induction region, the surface tension does not decrease significantly because the surfactant molecules have not diffused to the interface yet. Once in the fast-fall region, the surface tension decreases very quickly, and the rate of decrease reaches a maximum. In the plateau region, the surface tension values do not change much with time, and they eventually reach equilibrium. The rate of decrease of dynamic surface tension increases with an increase in the concentration of the surfactant, and with an increase in temperature at a fixed surfactant concentration. For an ionic surfactant, the rate increases with an increase in the electrolyte concentration of the solution. The induction period has previously been studied by Gao and Rosen (1995)

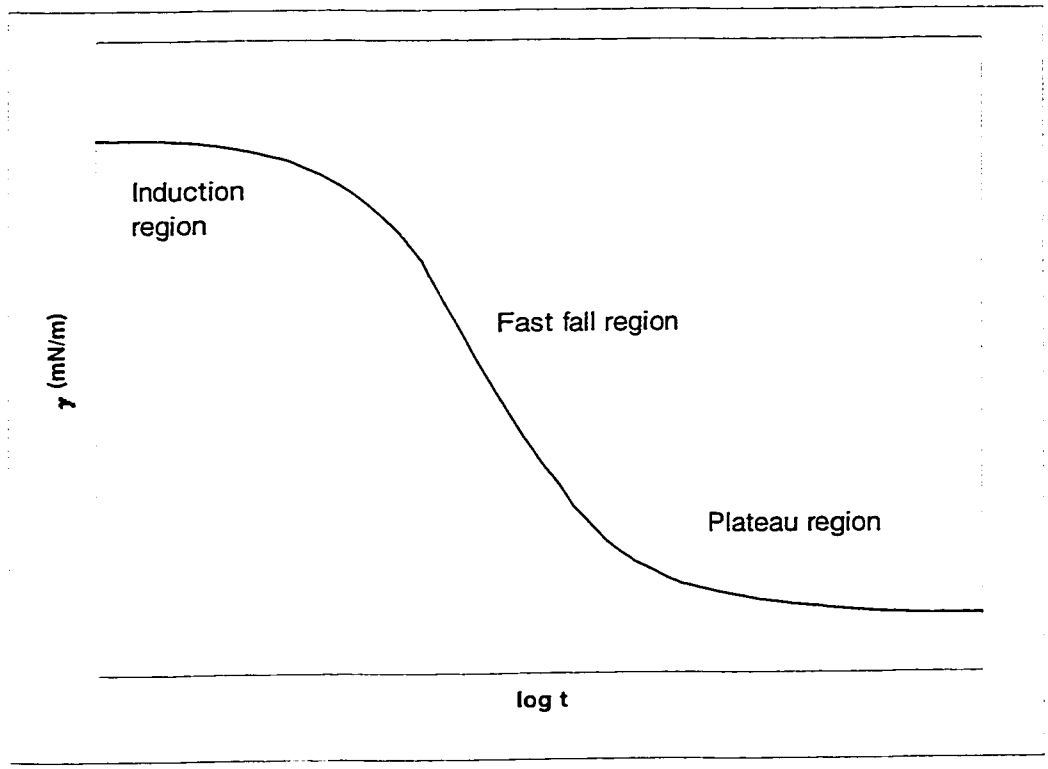

Figure 2.1 Generalized dynamic surface tension versus log time curve

using sodium dodecyl sulfate and polyoxyethylenated n-dodecyl alcohol solutions to understand the physical significance of dynamic parameters. They found that the dynamic surface tension is related to the difference between the energies of adsorption and desorption. The induction period is related to the surface coverage during the induction period so that surfactants with larger surface area per molecule decrease surface tension more rapidly than similar molecules with smaller surface area per molecule.

Tamura *et al.* (1995) studied the dynamic surface tension and foaming properties of aqueous polyoxyethylene n-dodecyl ether solutions. They found that for short surface formation times (<1s), the maximum rate of the decrease in the surface tension increased with an increase in ethylene oxide units. For longer formation times (>1s), when the dynamic surface tension approached the plateau region, the dynamic surface tension value in this region decreased with a decrease in ethylene oxide units.

2.2 Methods to Measure Dynamic Surface or Interfacial Tension

The measurement of interfacial tension is one of the most important experimental means of accessing the properties of an interface. When sorption processes are occurring, studying the time evolution of the dynamic interfacial tension may give important information about the surfactant, the interface and their interactions. There is a great variety of experimental methods for the study of dynamic surface and interfacial tension (Adamson, 1990). These methods will now be described briefly.

The maximum bubble pressure method is frequently used for the study of dynamic surface tension. This method is accurate to a few tenths of a percent. It does not depend on contact angle, and it requires only an approximate knowledge of the density of the liquid. Generally, the maximum bubble pressure apparatus consists of a gas-feeding system and a pressure and bubble rate measuring system. The gas is fed into the test liquid through sufficiently small tubes to give a great range in bubble formation times. The maximum bubble pressure method can be used only for dynamic measurements at the liquid / gas interface. Many reports have been published studying the dynamic surface tension of surfactant solutions by maximum bubble pressure. Hua and Rosen (1988) studied the basic parameters of dynamic surface tension of aqueous surfactant solutions by this method and first noted the four different stages of the dynamic surface tension versus log time curve already discussed. Dynamic surface tension and foaming properties of aqueous polyoxyethylene n-dodecyl ether solution were studied by Tamura *et al.* (1995). Miller *et al.* (1994) studied the dynamic effects of soluble adsorption layers. Recently, Fainerman and Miller (1995) have modified the maximum bubble pressure instrument so that bubble formation times close to 0.1 ms are now possible.

The drop weight method is one of the earliest methods of surface and interfacial tension determination (Adamson, 1990). The method is based on Tate's law:

$$w = 2 \pi r \gamma \qquad [2.1]$$

where w is the drop weight, r is the drop radius and γ is the surface or interfacial tension. This method may also be used for dynamic measurements. However, a correction factor usually has to be applied to get accurate results.

The de Nouy ring is a popular method for determining equilibrium surface and interfacial tension. In the method, the force exerted on a ring as it is pulled through a surface or interface is measured. Care must be taken to avoid any disturbance of the surface as the critical point of detachment is approached. The method is quite sensitive, but is not appropriate for determination of dynamic quantities.

The Wilhelmy plate method has been used since 1863(Adamson, 1990). This method is quite simple, and involves no corrections. The basic principle is that as a thin plate, such as a microscope cover glass or piece of platinum foil, is pulled through an interface, it will support a meniscus whose weight is given very accurately by the following equation:

$$W_{tot} = W_{plate} + \gamma p \qquad [2.2]$$

where W_{tot} is the total weight, W_{plate} is the weight of the plate, γ is the surface or interfacial tension, and p is the perimeter. Rosen and Gao (1995) have recently used the Wilhelmy plate technique to measure the equilibrium surface tension of several surfactant solutions.

The pendant drop method and sessile drop method both belong to the category of methods based on the shape of static drops or bubbles. The general procedure is to form the drop or bubble under conditions such that it is not subject to disturbances, and then to make certain measurements of its dimensions or its profile from a photograph, or through the use of a video. The direct fitting of the drop shape coordinates to the Gauss-Laplace equation is used to determine interfacial tension and contact angle. Usually, several tenths of a percent accuracy is attainable, and the method is well-suited to the observation of long-term change in interfacial tension. Bonfillon *et al.* (1994) have reported using the pendant drop method to determine the dynamic surface tension of ionic surfactant solutions. Nahringbauer (1995) studied the dynamic surface tension of aqueous polymer solutions by the same method. The pendant drop method can also be used to measure the dynamic values at liquid-liquid interfaces.

One of the oldest experimental techniques for the measurement of surface tension is the oscillating jet method. The idea is based on the analysis of a stationary jet issuing from a capillary which oscillates about its equilibrium section into the atmosphere. The oscillating jet method provides dynamic surface tensions in a time interval from 3 ms to 50 ms, and has been used by many authors. Rillaerts and Joos (1982) have used this method to determine the rate of demicellization from dynamic surface tension data of micellar solutions of Triton X-100 and cetyltrimethylammonium bromide.

Van Uffelen and Joos (1994) have recently proposed a new method of surface tension measurement called "peak tensiometry". It is based on the measurement of the dynamic

surface tension of a linearly expanded solution / air surface. The apparatus consists of a trough which is filled with a surfactant solution. A barrier rests on the upper side of the trough, and divides the solution / air surface into two separate parts. The barrier can be moved at a constant speed along the whole length of the trough. The method allows the study of a wide range of surfactant concentrations from well below cmc up to concentrations well above cmc with a glass barrier. This instrument has been used to study the dynamic surface tension of decanoic acid, Triton X-100, and Brij 58 (Horozov and Joos, 1995).

The drop volume method is one of the most widely used interfacial tension measurement techniques. In this method, the volume of a drop detaching from a capillary is used to calculate interfacial tension. Typical instruments require correction factors which depend both on the capillary diameter and the drop volume. Recent instruments which make use of extremely small capillaries, avoid the need for these empirical corrections. The method is very convenient for measuring dynamic surface and interfacial tensions. More importantly, this method is well-suited to comparing individual surfactants and for evaluating surfactant blends for optimum properties. The instrument used in this research work is based on the drop volume method, and is described in the experimental procedure section in greater detail. Xu (1995) used this method to study the dynamic interfacial tension between bitumen and aqueous sodium hydroxide solutions. He found that for optimum bitumen recovery, the capillary number is a critical parameter. Van Hunsel *et al.* (1986) studied the adsorption kinetics at the oil / water interface by this method. More recently, Molley *et al.* (1996) used this apparatus to compare the effect of ready-made

and *in-situ*-formed surfactants on dynamic interfacial tensions. In their study, the dynamic interfacial tension of sodium linoleate dissolved in an aqueous phase was measured and compared with the dynamic values obtained by adding linoleic acid in the oil phase, and NaOH in the aqueous phase.

Miller *et al.* (1994) compared four experimental methods for the measurement of dynamic surface tension of surfactant solutions. The drop volume method, maximum bubble pressure method, oscillating jet method and inclined plate method were all found to produce consistent results. To study the dynamics of adsorption in a time interval from a few milliseconds up to some minutes, the drop volume and the maximum bubble pressure methods are particularly effective. Comparison with the remaining two methods gave very good agreement, even in the milliseconds time range. Thus, for studies involving dynamic surface or interfacial tension, an important parameter to consider when selecting a measurement technique is the range of interface formation times of interest.

2.3 Surfactants and Surfactant Classification

Surfactants possess a characteristic chemical structure that consists of a hydrophobic moiety, or tail, and a hydrophilic moiety, or head. Materials that possess chemical groups leading to surface activity are generally referred to as being amphiphilic, indicating that they have some affinity for two essentially immiscible phases. The amphiphilic structure of surfactant molecules results in the adsorption of surfactants at interfaces, and the

consequent alteration of the corresponding interfacial energies. It also results in the orientation of the adsorbed molecules such that the hydrophobic tails are directed away from the bulk solvent phase. The resulting molecular orientation produces some of the most important microscopic effects observed for surface-active materials.

Synthetic surfactants and the natural fatty acid soaps are typical amphiphilic materials that tend to exhibit some solubility in water, as well as some affinity for non-aqueous solvents. As a basis for understanding the relationship between surfactant structures and surface activity, it is useful to consider how changes in the polarity of a specified hydrocarbon chain affects its solubility and surface activity. As an illustration, consider the straight-chain hydrocarbon dodecane, $CH_3(CH_2)_{10}CH_3$, a material that is, for all practical purposes, insoluble in water. If a terminal hydrogen in dodecane is exchanged for a hydroxyl group, the new material, n-dodecanol, $CH_3(CH_2)_{10}CH_2OH$, still has very low solubility in water, but the tendency toward solubility has been increased substantially, and the material begins to exhibit characteristics of surface activity. If the alcohol functionality is placed internally on the dodecane chain, as in 3-dodecanol, the resulting material will be similar to the primary alcohol, but will have slightly different solubility characteristics (slightly more soluble in water). Those differences will generally be carried over in differences in surface activity. The effects of the position of substitution on surfactant properties can be quite large.

Surfactants may be classified in several ways, depending on the intentions and preferences of an author or user. One of the more common schemes relies on

classification by the application under consideration, so that surfactants may be classified as emulsifiers, foaming agents, wetting agents, dispersants, and so on.

In aqueous systems, which constitute by far the largest number of surfactant applications, the hydrophobic group generally includes a long-chain hydrocarbon radical, although there are examples of compounds containing halogenated or oxygenated hydrocarbons, or siloxane chains. The hydrophilic group will be an ionic or highly polar group that can impart some water solubility to the molecule. So a very useful chemical classification of surface-active agents is based on the nature of the hydrophile, with subgroups being defined by the nature of the hydrophobe. The four general groups of surfactants are defined as follows:

1. anionic, with the hydrophilic group carrying a negative charge such as carboxyl, sulfonate, or sulfate;
2. cationic, with the hydrophilic group bearing a positive charge, as for example, the quaternary ammonium halides;
3. nonionic, where the hydrophile has no charge, but derives its water solubility from highly polar groups such as polyoxyethylene or polyol groups;
4. amphoteric, in which the molecule contains, or can potentially contain, both a negative and a positive charge, such as the sulfobetaines, $R^{+}(CH_3)_2CH_2CH_2SO_3^{-}$.

Most published research has studied nonionic or anionic surfactants. These two types of surfactants are the most common in soil decontamination applications (Ouyang, 1995;

Adeel and Luthy, 1995). In recent years, research is increasingly focused on surfactant mixtures and their interactions. Rosen and Gao (1995) studied mixtures of differently charged surfactants, including: $C_{12}SNa$, $C_{12}EO_7$, $C_{14}N(CH_3)_2O$, and $C_{12}PyrBr$. They used a maximum bubble pressure apparatus to measure the dynamic surface tension. Different adsorption models were used to interpret the experimental data. The diffusion coefficients, calculated from the adsorption models, decrease with an increase in the strength of the interaction between the two surfactants. When there is strong interaction between the two surfactants in a mixture, the system showed higher surface tension at short adsorption time than for any of individual components present in the mixture. At long adsorption time, the result is reversed. For weakly interacting mixtures, the surface tension of the mixture approximates that of the more surface active component at short adsorption time. At longer adsorption times the surface tension approaches the lowest equilibrium value of the individual compounds.

2.4 Adsorption Kinetics of Surfactants

If a bulk phase in a two phase system contains surfactant, the surfactant molecule will diffuse from the bulk phase to the interface as interfacial area is formed due to the amphiphilic nature of the surfactant. The time required for the surfactant molecules to be transported from the bulk phase to the interface, as well as the number of surfactant molecules that can be adsorbed at the interface, will depend on the nature of the surfactant. These parameters can be determined by studying the adsorption kinetics of surfactants. Generally, the adsorption of a surfactant consists of two steps: a diffusion

step followed by a transfer step (Miller and Kretzschmar, 1991). Figure 2.2 shows a schematic representation of the adsorption process. In the diffusion step, the surfactant molecules diffuse from the bulk phase to the subsurface layer due to a concentration gradient. In the transfer step, the surfactant molecules are transfered from the subsurface to the interface, or in other words, from the solved state to the adsorbed state. Once the surfactant molecules are adsorbed at the interface, desorption processes will also occur. Depending on the surfactant interfacial concentration, the adsorption kinetics of surfactant molecules can be adsorption dominant, desorption dominant, or at equilibrium when the adsorption rate is equal to the desorption rate.

The basic relationship that governs the adsorption of surfactant molecules is the Gibbs adsorption isotherm. It relates the surface excess concentration of the adsorbed species to the surface or interfacial tension. The Gibbs isotherm can be written as:

$$\Gamma = -\frac{1}{RT}\frac{d\gamma}{d\ln C} \qquad [2.3]$$

Where Γ is the surfactant interfacial concentration, T is the absolute temperature, and C is the surfactant bulk concentration. Since the Gibbs equation relates the surface excess concentration of the adsorbed species to the surface or interfacial tension, the measurement of dynamic surface or interfacial tension can in theory be used to study adsorption kinetics.

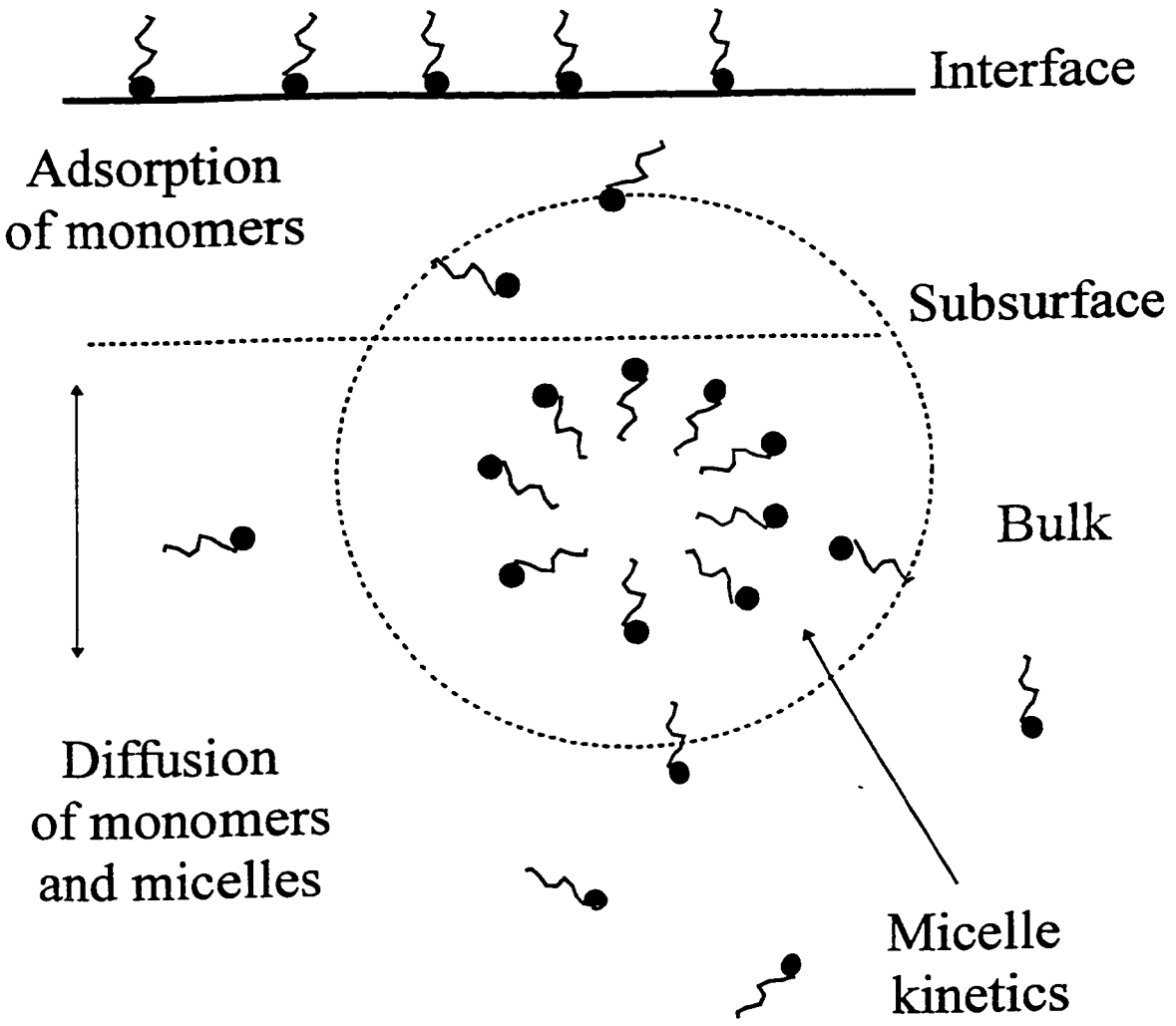

Figure 2.2 Schematic representation of the surfactant adsorption process

One of the specific properties of surfactants is that they form micelles once a certain concentration, the cmc, is reached. The shape and the size of the micelles depend on the structure and length of the molecules. Co-surfactants such as alcohols may have a great effect on micelles, and consequently on surface and interfacial tension. Forland *et al.* (1994) studied the effect of medium chain length alcohols on the micellar properties of sodium dodecyl sulfate in sodium chloride solutions. They found that short and medium chain length alcohols may lead to a decrease in the micellar size. On the other hand, addition of medium to long chain alcohols increased the aggregation number, producing larger alcohol-surfactant mixed micelles. Addition of alcohols apparently affected micelles in two ways: by their effect on water, and by their effect on solubility. For the lower homologues, the effect on water was dominant, leading to a break-down of the micellar structure. For the higher homologues starting with pentanol, solubilization outweighed the effect on water, the overall result being increased micellar size. At higher concentrations, far beyond the cmc, the phase behavior was found to be much more complex.

The presence of micelles in the bulk solution can influence the adsorption kinetics remarkably. The effect may be explained in the following way. After a fresh surface has been formed, surfactant molecules are adsorbed, resulting in a concentration gradient of monomers. This gradient will be equalized by diffusion to re-establish a homogeneous distribution. Simultaneously, the micelles are no longer in equilibrium with monomers in the bulk solution. This leads to a net process of micelle dissolution, or rearrangement to

re-establish the local equilibrium. As a consequence, a concentration gradient of micelles results, which is equalized by the diffusion of micelles. On the basis of this idea, it is expected that the ratio of monomers to micelles, the aggregation number, rate of micelle formation and dissolution, will all influence the rate of adsorption processes. Figure 2.2 illustrates this phenomenon. Clearly, the transport of monomers and micelles, as well as the mechanism of micelle kinetics, have to be taken into account in a reasonable physical model of adsorption above the cmc.

To account for the effect of micelles, it is necessary to account for the various mechanisms as illustrated in Figure 2.3 (Dukhin, 1995). The formation-dissolution model shown in mechanism 1 assumes a total dissolution of a micelle in order to re-establish the local equilibrium monomer concentration. This model is based on an idealized distribution of only monomers and micelles with a definite aggregation number. Mechanism 2 is based on the existence of micelles of different size and therefore, a broad micelle size distribution has to be assumed. Model 3 is the most complex one. It allows the aggregation or dissolution of individual monomers to or from the micelles. If a micellar size distribution is assumed, based on experiments, a large number of formation and dissolution rate constants accounting for each micellar size must be obtained. These models provide an illustration of the problems encountered in attempting to model surfactant adsorption processes above the cmc.

The adsorption kinetics of an acidified oil / surfactant system was studied by Touhami *et al.* (1994). They demonstrated that the predominant enhanced oil recovery techniques for

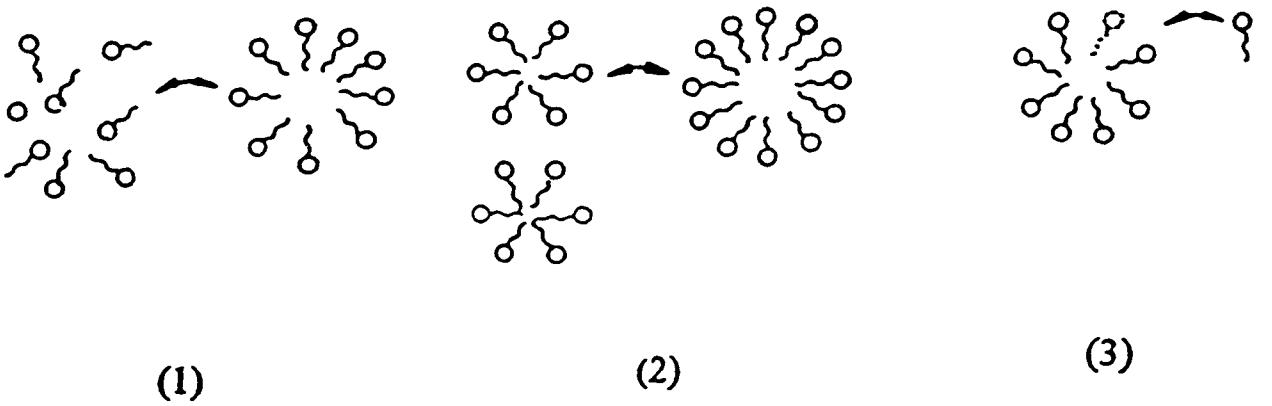

Figure 2.3 Schematic representation of various micelle formation-dissolution mechanisms (from Dukhin *et al.*, 1995)

achieving low interfacial tension are micellar and alkaline flooding. Their studies showed that the interactions between surfactant / alkaline mixtures and acidic oil exhibited a marked synergistic effect on interfacial tension reduction. The magnitude of this effect was found to vary not only with the oil acidity, alkali concentration and salinity, but also with the surfactant concentration and type. In their paper, linoleic acid was dissolved in light paraffin oil and sodium dodecyl sulfate was used as a surfactant. The addition of linoleic acid to paraffin oil resulted in significantly reduced interfacial tension of the oil against water. Interfacial tension reductions observed for acidified paraffin oil against sodium dodecyl sulfate solutions were greater than those observed with acid or surfactant only. This study showed the importance of surfactants dissolved in both phases in order to achieve greater reduction in interfacial tension.

Another quite important type of adsorption behavior results from the electrical repulsion in adsorption layers of ionic surfactants. The adsorption of ionic surfactants at a surface or interface leads to the build-up of a surface charge. Thus, the kinetics of adsorption are coupled with the formation of an electrical double layer at the interface. There is evidence that the electrical double layer can retard the adsorption flux of the surfactant ions because of a growing electrostatic barrier (Dukhin *et al.*, 1995).

2.5 Surfactant Adsorption Models

In order to describe the adsorption behavior of surfactants, different adsorption models have been developed. Since the adsorption of a surfactant is an activated process in which molecules are transported to the surface both by the diffusion of molecules in the bulk phase, and by overcoming an energy barrier which may be present at the interface (Miller and Kretzschmar, 1991), two different kinds of adsorption models are typically used. When the adsorption is limited by the diffusion of surfactant molecules from the bulk phase to the subsurface layer, the surfactant adsorption is said to be diffusion-controlled. When the adsorption is limited by the transfer of surfactant molecules from the solved state to the adsorbed state, the surfactant adsorption is said to be kinetic-controlled.

To develop appropriate models for surfactant adsorption, it is necessary to know the time available for adsorption, t_a. In a drop volume tensiometer, the drop formation time, t, is measured directly. However, t is larger than t_a because of the continuous growth of the drop. Previous experimental studies have shown that the two parameters are related through the following equation (Dukhin *et al.*, 1995; Van Hunsel *et al.*, 1986):

$$t_a = 3/7t \approx 0.43\ t \qquad [2.4]$$

2.5.1 Diffusion-Controlled Models

The classical form of the diffusion controlled adsorption equation has been derived by

Ward and Tordai (1946). It is based on the assumption that the interfacial concentration of surface active molecules, Γ, is limited by diffusion of the surfactant from the bulk phase. The mathematical expression has the following form:

$$\Gamma(t_a) = 2\sqrt{\frac{D}{\pi}}\left(C_0\sqrt{t_a} - \int_0^{\sqrt{t_a}} c(0, t_a - \lambda)d\sqrt{\lambda}\right) \qquad [2.5]$$

where $\Gamma(t_a)$ is the dynamic surfactant interfacial concentration, C_0 is the surfactant bulk concentration, c is the surfactant subsurface concentration, D is diffusion coefficient, λ is a dummy variable for a constant interfacial area, and t_a is the adsorption time. For a growing drop, the adsorption time is given by Equation [2.4]. Miller and Kretzschmar (1991) derived the adsorption kinetics for a growing drop using Equations [2.4] and [2.5], and obtained the following result (Miller and Kretzschmar, 1991):

$$\Gamma(t) = 2C_0\sqrt{\frac{3Dt}{7\pi}} - \sqrt{\frac{D}{\pi}}t^{-2/3}\int_0^{\frac{3}{7}t^{7/3}} \frac{c(0, \frac{7}{3}\lambda^{3/7})}{(\frac{3}{7}t^{7/3} - \lambda)^{1/2}}d\lambda \qquad [2.6]$$

2.5.1.1 Short Diffusion Time Approximation

In the beginning of the adsorption process the subsurface concentration is small. The second term of Equation [2.6] can be neglected, and the equation becomes:

$$\Gamma(t) = 2C_0\sqrt{\frac{3Dt}{7\pi}} \qquad [2.7]$$

An isotherm is required to relate Γ to γ. The Langmuir-Szyszkowski equation has been shown to be valid under a variety of experimental conditions (Horozov and Joos, 1995; Rillaerts and Joos, 1982). This equation can be written as:

$$\Gamma(t) = \Gamma_\infty\left\{1-\exp\left[\frac{\gamma(t)-\gamma_0}{RT\Gamma_\infty}\right]\right\} \qquad [2.8]$$

Where Γ_∞ is the maximum surfactant interfacial concentration, and γ_0 is the interfacial tension of the pure interface. Substituting Equation [2.8] into Equation [2.7] gives:

$$\gamma(t)-\gamma_0 = RT\Gamma_\infty \ln\left(1-\frac{2C_0}{\Gamma_\infty}\sqrt{\frac{3Dt}{7\pi}}\right) \qquad [2.9]$$

Equation [2.9] can be further simplified by assuming ln (1-X) = -X, when $0 < X < 0.5$, to give, finally:

$$\gamma(t)-\gamma_0 = -2RTC_0\sqrt{\frac{3Dt}{7\pi}} \qquad [2.10]$$

Equation [2.10] is expected to be valid for short surfactant diffusion times.

2.5.1.2 Long Diffusion Time Approximation

When the adsorption process is near equilibrium, Equation [2.6] can be simplified to (Joos *et al.*, 1992):

$$\Gamma(t) = 2\Delta C_s\sqrt{\frac{3Dt}{7\pi}} \qquad [2.11]$$

with $\Delta C_s = C_0 - c$. Because the adsorption process is diffusion-controlled, this change in the subsurface concentration will correspond to a change in interfacial tension (Joos *et al.*, 1992) so that:

$$\gamma - \gamma_e = \frac{d\gamma}{dC}\Delta C_s \qquad [2.12]$$

Introducing Gibbs' equation, Equation [2.3], and Equation [2.12] into Equation [2.11] gives:

$$\gamma = \gamma_e + \frac{RT\Gamma^2}{C_0}\sqrt{\frac{7\pi}{12Dt}} \qquad [2.13]$$

Equation [2.13] is expected to be valid when the adsorption process is near equilibrium; that is, for long diffusion times.

If the surfactant adsorption process is diffusion-controlled, a plot of interfacial tension versus either square root of drop formation time or one over square root of drop formation time should give a straight line with the slope related to the diffusion coefficient, depending upon which approximation is valid.

2.5.1.3 Characteristic Diffusion Time

In order to determine whether the short or long diffusion time approximation is valid, it is necessary to compare the time available for adsorption to a characteristic diffusion time for the surfactant of interest. An equation defining a characteristic diffusion time, τ_D, for

surfactants has been previously proposed (Dukhin *et al.*, 1995; Joos and Van Uffelen, 1995), and is given by:

$$\tau_D = \frac{1}{D}\left(\frac{d\Gamma}{dC_o}\right)^2 \qquad [2.14]$$

The differential term can be evaluated through the use of an appropriate equation of state. The ratio of adsorption time, t_a, to τ_D should thus be an important parameter in modeling the diffusion-controlled adsorption of surfactants.

2.5.2 Kinetic Controlled Model

For kinetic-controlled adsorption, the most frequently used rate equation is based on the Langmuir mechanism, which reads in its general form:

$$\frac{d\Gamma}{dt} = k_{ad} C_0 \left(1 - \frac{\Gamma}{\Gamma_\infty}\right) - k_{des}\Gamma \qquad [2.15]$$

In Equation [2.15], k_{ad} is the surfactant adsorption rate constant, and k_{des} is the surfactant desorption constant rate. Under the condition $\Gamma / \Gamma_\infty << 1$, i.e. at small interfacial coverage, the so-called Henry mechanism results,

$$\frac{d\Gamma}{dt} = k_{ad} C_0 - k_{des}\Gamma \qquad [2.16]$$

This equation has been shown to have general validity for kinetic-controlled adsorption of low concentrations of surfactants.

2.6 Dynamic Interfacial Tension and Surfactant Adsorption Models

Due to the growing interest in surfactant adsorption kinetics, many types of models have been developed and tested for different types of surfactants. Some of these models have been developed especially for oil / water interfaces.

The adsorption of most nonionic surfactants studied in the literature can be described adequately by considering diffusion-controlled models alone. Van Hunsel *et al.* (1986) used Triton X-100 and Brij 58 to study the adsorption kinetics of surfactants at the oil / water interface. They found that when the surfactant is dissolved in the aqueous phase and insoluble in the oil phase, the adsorption kinetics at the air / water and oil / water interface were equivalent, and that the surfactant adsorption was diffusion controlled. When the surfactant was dissolved in the oil phase, and nearly insoluble in the water phase, long time effects were observed. These effects could not be explained by either diffusion nor kinetic models, but were attributed to a reaction at the interface.

The adsorption of Triton X-100 at the n-hexane / water interface was also studied by Liggieri *et al.* (1995) using a capillary pressure method. The results of this study showed that the adsorption was, essentially, diffusion-driven. From the measurements of the dynamic interfacial tension, it was possible to conclude that the adsorption potential barriers were negligible, and to calculate the diffusion coefficient.

Even for diffusion-controlled adsorption, the model used to describe the adsorption may differ depending on the instrument used for the dynamic interfacial tension measurement. Joos and Van Uffelen (1995) developed a model based on diffusion-controlled adsorption kinetics to interpret the dynamic interfacial tension obtained by the growing drop technique. They found that the model applied when certain experimental conditions were met. These conditions included: that the experiment started from an equilibrium state; that the interface expansion rate was known; that at the beginning, the drop was spherical; and that the jumps in interfacial tension were small. Triton X-100 was used to test this model, and the agreement between the experiments and the theory was found to be satisfactory.

When ionic surfactants are used, the adsorption potential barrier can not be neglected anymore, and adsorption kinetics become more complicated. For different adsorption times, the rate-limiting step may be different. Sodium dodecyl sulfate and sodium dodecyl benzene sulfate solutions were used to study the dynamic interfacial tension of ionic surfactant solutions (Bonfillon *et al.*, 1994). It was found that for ionic surfactants, the initial adsorption stage is controlled by surfactant diffusion to the interface. The adsorbed surfactant ions then produced an increasing electrostatic potential, which slowed down the adsorption of new surfactant ions. At an intermediate level of adsorption, the potential was strong enough to stop the adsorption process.

In some cases, the surfactant adsorption is neither diffusion controlled, nor kinetic controlled, but rather controlled by a combination of the two mechanisms. Adamczyk (1987) developed a theoretical prediction for adsorption kinetics under these circumstances. The dynamic surface tension of 1-9-nonanediol solutions was measured by the oscillating-jet method to test the theoretical predictions. The theoretical results, obtained by a numerical solution of the adsorption equations, agreed well with the experimental data. At the same time, the author demonstrated that an approximate kinetic equation derived by Joos *et al.* for purely barrier-controlled adsorption was less accurate.

In 1993, Ravera *et al.* developed a theoretical approach for sorption kinetics in which adsorption-desorption is considered to be an extended diffusion process with a renormalized diffusion coefficient taking into account an interfacial potential barrier. This model allowed the description of the time dependence of the process by considering both the crossing of an interfacial potential barrier, and diffusion into the neighboring phase. Their model led to an expression for the surface concentration as a function of time, and of the molecular activation energies of adsorption and desorption. However, this new model was only derived for the gas / liquid interface.

Ravera *et al.* (1994) improved their model to study the sorption kinetics at liquid-liquid interfaces with surfactant soluble in both phases. This new extension in their former theoretical approach allowed the study of the adsorption kinetics in the presence of the adsorption barrier in terms of a renormalized diffusion process. It was thus possible to solve the problem of adsorption with diffusion occurring in both of the phases in contact.

Chapter 3. Research Objectives

Many different technologies have been used to remediate contaminated soil. Among these technologies, surfactant-enhanced remediation is of growing importance, especially for hydrophobic organic compounds. Surfactants can be used to increase the solubility of HOCs, or they can be used to enhance the mobilization of organic compounds.

Although surfactant-enhanced soil remediation has been used more and more widely, the technology is still not well understood from a theoretical viewpoint, especially for surfactant-enhanced mobilization processes. Experimental studies to date have shown that the mobilization of soil contaminants occurs under dynamic conditions, and the efficiency can be improved by optimizing the use of surfactants. In practice, experimentation with different types and different concentrations of surfactants for specific soil contaminants is required to optimize the recovery process in each case. This approach is extremely time consuming, and in some cases, the recovery of HOCs is far from satisfactory. Thus, specific knowledge of the dynamic adsorption behavior of surfactants is of great interest to characterize surfactants for soil remediation. The research objectives of this work can be summarized as follows:

- to develop a method for using a drop volume tensiometer to study the dynamic interfacial tension at liquid-liquid interfaces for application to both light and dense non-aqueous phase liquid contaminants;

- to measure the interfacial tension of selected synthetic surfactants at the mineral oil-water interface;
- to fit appropriate adsorption models to the dynamic interfacial tension data obtained;
- to explain the adsorption behavior of the selected surfactants using consistent adsorption mechanisms;
- to study the influence of adsorption time on the two commonly used approximations of the diffusion-controlled model.

Chapter 4. Experimental

All experiments were conducted with the DVT-10 drop volume tensiometer. Several different organic phases and surfactants were tested. These materials are described in detail below.

4.1 Materials

The aqueous phases for all experiments were made with deionized water. The non-aqueous phases tested included the following organic compounds: dodecane, carbon tetrachloride, and a light, white mineral oil. The properties of these three organic compounds are summarized in Table 4.1.

Three synthetic surfactants were selected, and tested as received. Sodium dodecyl sulfate (SDS) was obtained from Fisher Scientific Ltd. and was supplied as a powder. SDS is an anionic surfactant readily soluble in the water phase. The molecular weight of SDS is 288 g/mol.

Span 80 (sorbitan monooleate) was obtained from Sigma Chemical Co. Span 80 is a non-ionic surfactant that contains a mixture of fatty acid components in addition to the predominant oleic acid component. The density of Span 80 was measured as 999 kg/m^3 at room temperature. In all concentrations tested, Span 80 was readily soluble in the oil

Table 4.1

Properties of Organic Compounds Used in This Research

Organic Compound	Density (kg/m^3)	Viscosity (mPa s)	Supplier
dodecane	750	--	Sigma Chemical Co.
carbon tetrachloride	1587	--	Fisher Scientific Ltd.
mineral oil	862	22.7	Sigma Chemical Co.

Note: All the values were measured at $21\pm1^{0}C$.

phase, and the nominal value of the molecular weight is 428 g/mol (Span 80 Product Information Bulletin, 1996).

Triton X-100 (octylphenoxypolyethoxyethanol), obtained from Sigma Chemical Co., is also a non-ionic surfactant, but is soluble in the water phase. The surfactant has a density of 1070 kg/m^3 at room temperature, and a molecular weight of 647 g/mol.

It should be mentioned that Triton X-100 and Span 80 are in fact mixtures. However, no minimum has been observed in the equilibrium interfacial tension versus concentration curves at cmc, indicating that highly surface active minor components are absent. The recent study by Horozov and Joos (1995) with Triton X-100 did not show any peculiarities of its surface properties. That is why it is believed that both Triton X-100 and Span 80 can be treated as pure compounds with respect to their surface properties.

The three selected surfactants represent some of the typical cases often encountered in surfactant-enhanced soil remediation: namely, anionic surfactant in aqueous phase; non-ionic surfactant in an aqueous phase; and non-ionic surfactant in an oil phase. This selection of surfactants allowed the study of different adsorption mechanisms to be possible.

4.2 Apparatus

All interfacial tension measurements were made with the DVT-10 drop volume tensiometer, manufactured by Krüss. The DVT-10 consists of a control and data reduction module, and a sample cell including a capillary and photocell assembly. A syringe pump is also required to operate the unit. The controller is menu or computer driven, asking for input on sample density, flow rate, and number of drops to be counted. Dynamic interfacial tension data are calculated as each drop detaches, along with statistics for the experiment. A range of syringe sizes can be used in the pump, although the 0.10, 0.25, 0.50 and 1.00 mL volumes produce data with the lowest relative standard deviation. In all the experiments in this research work, a 0.25 mL syringe is used.

Figure 4.1 shows a schematic representation of the sample cell. One liquid phase is placed in the glass tube. The second liquid is introduced into the tube through a 254 μm capillary by using the syringe pump. The capillary can be attached to the tube either at the top, or at the bottom. This allows two possible capillary orientations: vertically up (Figure 4.1A), thus allowing the introduction of the light phase into the heavy phase; or vertically down (Figure 4.1B), thus allowing the introduction of the heavy phase into the light phase. In the following sections of this work, the configuration represented by Figure 4.1A will be referred to as configuration A, while the configuration represented by Figure 4.1B will be referred to as configuration B. An infrared light emitting diode and photodiode are positioned about half-way along the glass tube in order to detect the drops

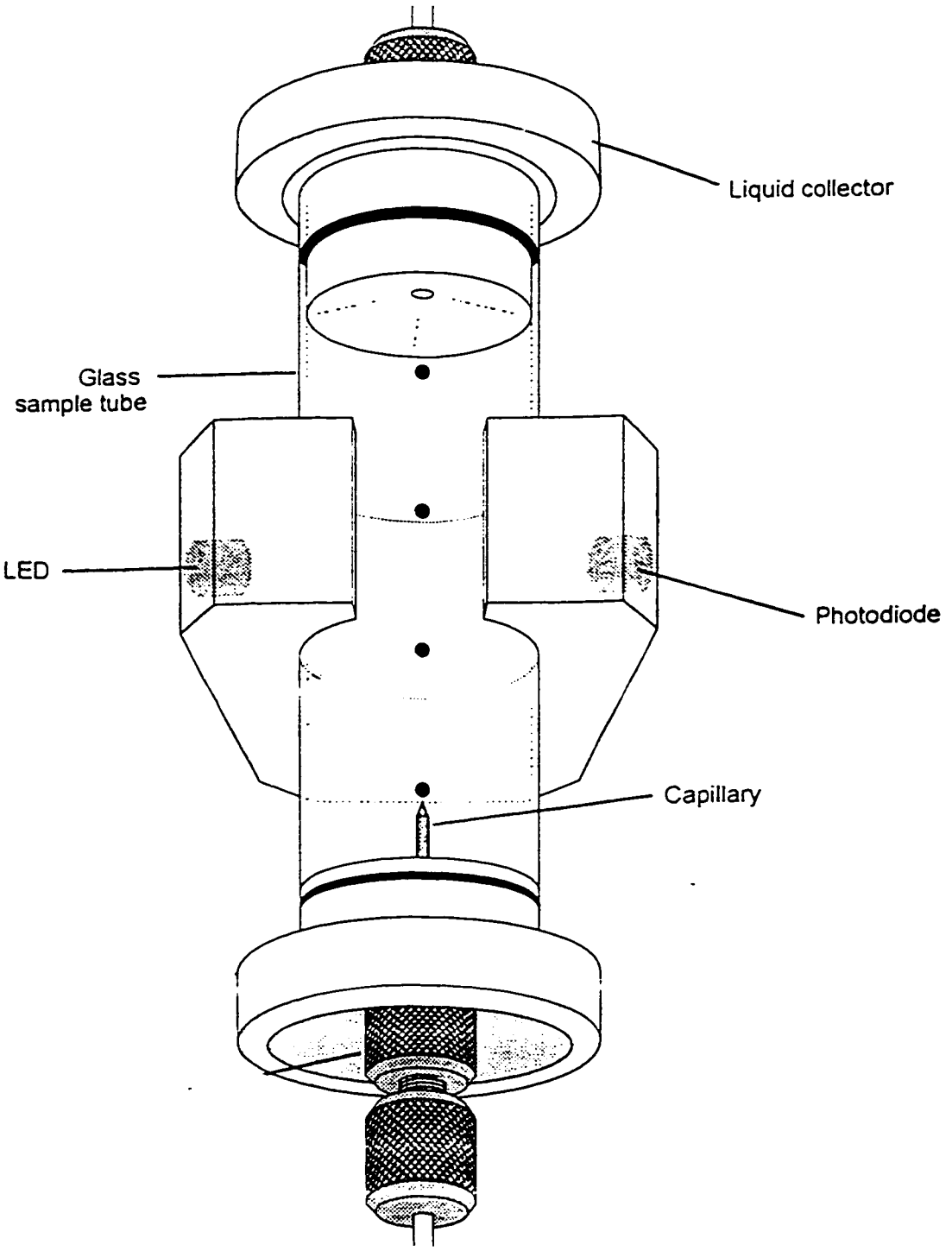

Figure 4.1A Schematic representation of the sample cell: capillary orientation A

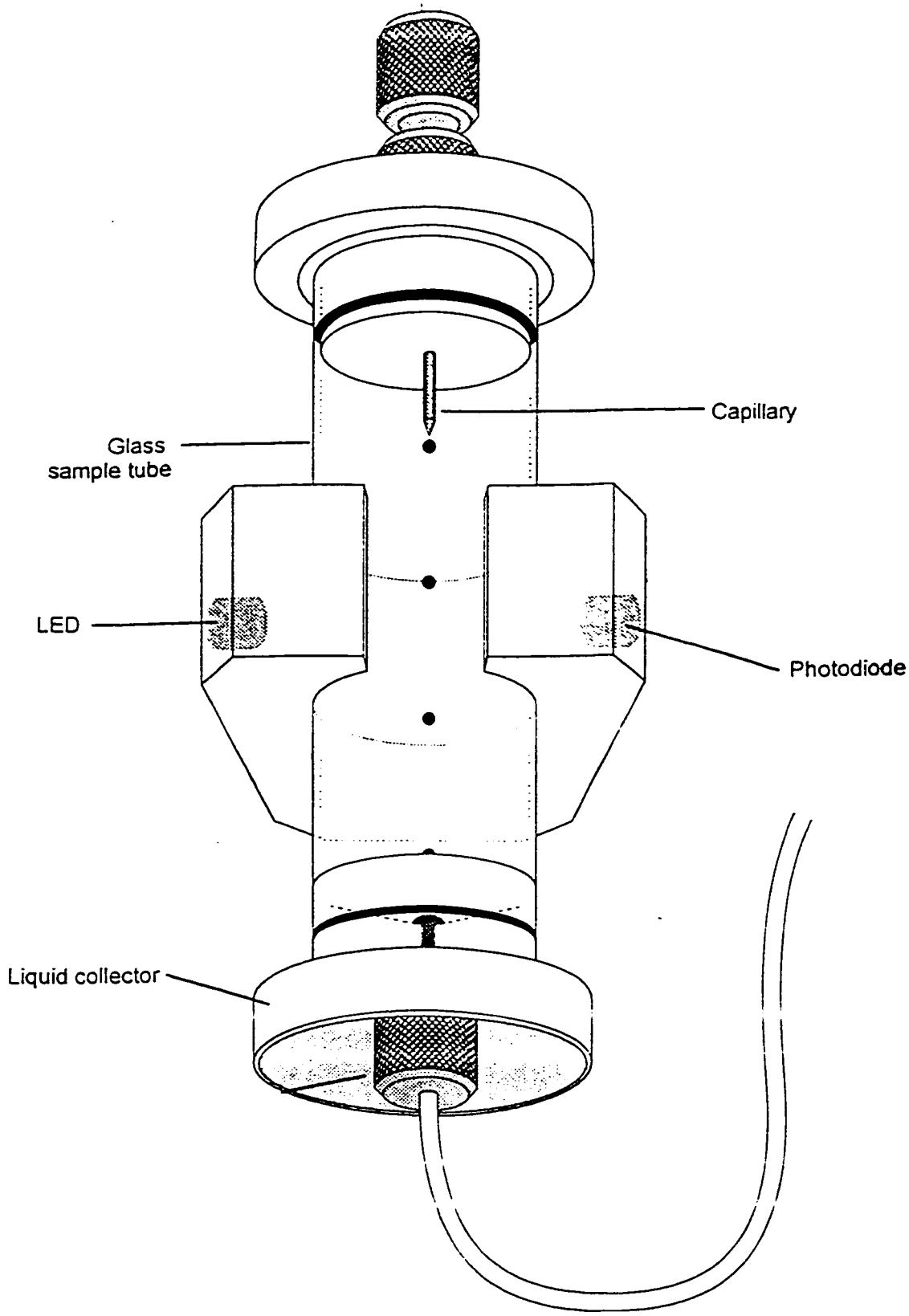

Figure 4.1B Schematic representation of the sample cell: capillary orientation B

as they detach from the capillary. A timer is started when the first drop is detected. Elapsed times between subsequent drops are then measured. Since the flow rate is kept constant by the syringe pump, the time between drops can be used to calculate the volume of each drop.

A force balance on a drop ready to detach at the tip of the capillary orifice results in the following equation for interfacial tension:

$$\gamma = \frac{V(\varrho_H - \varrho_L)g}{\pi d} \qquad [4.1]$$

In Equation [4.1], V is the volume of the drop, ϱ_H and ϱ_L are the densities of the heavy phase and light phase, respectively, and d is the orifice diameter of the capillary. The wall thickness at the tip of the capillary is 5 μm. This thickness is sufficiently small that the usual corrections for the wetting of a blunt tip are not required in the DVT-10 for the capillary size used (Xu, 1995; Hool and Schuchardt,1992).

4.3 Experimental Procedure

Since SDS was supplied as a powder, an analytical balance was used to weigh the quantities to be used in aqueous solutions. The known weight of SDS powder was added to a known volume of deionized water in a volumetric flask at room temperature to obtain concentrated solutions. The concentrated solutions were allowed to equilibrate in the laboratory for 24 h, and were subsequently diluted by adding different volumes of deionized water to obtain the final concentrations for testing.

Triton X-100 was supplied as a liquid. A known volume of the surfactant was added with a pipette to a known volume of deionized water to make concentrated solutions. These solutions were then diluted to obtain the concentration required for testing. The density of Triton X-100 was measured at room temperature with a pycnometer. By using the density and the molecular weight, it was thus possible to express Triton X-100 concentrations in units of mmol/L. A similar procedure was used for the preparation of Span 80 solutions except that Span 80 was dissolved in a known volume of mineral oil.

All the chemicals used in the experiments were allowed to stand at room temperature for at least 48 h prior to testing in the tensiometer. Before testing, the test samples were all stirred to ensure complete dissolution of the surfactants, and then allowed to stand at room temperature.

The density of mineral oil, Span 80 and Triton X-100 was measured with a pycnometer using the following procedure. First, the empty pycnometer was weighed on the analytical balance. Then, deionized water was added to the pycnometer, and the weight was measured again. The weight of the water was obtained by subtracting the latter weight from the former weight. The pycnometer was cleaned and dried. The liquid to be tested was introduced into the pycnometer and weighed again. The test liquid weight was obtained by subtracting the pycnometer weight. Since the volume is the same,

$$\varrho_t/m_t = \varrho_w/m_w \qquad [4.2]$$

where the w subscript refers to water, and the t subscript refers to the test liquid. Since the density of water is known, the density of the test liquid is easily calculated from the above equation.

The viscosity of mineral oil was measured with a kinematic viscometer. Before measuring, the viscometer was cleaned with suitable solvents, and then by passing clean, dry air through the instrument to remove the final traces of solvents. The sample was then charged into the viscometer, and the viscometer was placed into a holder and inserted into a constant temperature bath for 10 minutes. Suction was applied to draw the oil slightly above the measuring section of the viscometer. The efflux time was then measured by allowing the oil sample to flow freely out of the measuring section. Finally, the viscosity of the mineral oil was calculated by multiplying the efflux time by the viscometer constant.

The tensiometer was cleaned thoroughly prior to the start of each experiment. The light and heavy phases to be tested were introduced either into the glass tube or into the syringe depending on the experimental configuration employed. Any air bubbles present in the syringe pump tubing were removed by operating the pump. The capillary was then attached to the glass tube in the appropriate configuration depending on the experiment to be performed.

A constant flow rate was selected for the syringe pump at the start of each experiment. For each flow rate tested, the volumes of at least five drops were measured, and an average value was used in subsequent calculations. Five different flow rates were chosen, ranging from 0.1 mL/h to 1.0 mL/h. In all the experiments reported here, the relative standard deviation (which is 100 times the standard deviation divided by the mean) was below one. All measurements were carried out at 21±1°C.

Selected experiments were recorded with an 8 mm Sanyo video camera equipped with a macro lens. These video tapes allowed a closer examination of the neck formation mechanism. By viewing individual frames, it was also possible to obtain approximate values of physical characteristics, such as the length and diameter of the neck during the various phases of the drop growth.

.

Chapter 5. Procedure for Tensiometer Data Interpretation

This section deals with the novel procedure developed to interpret data from the DVT -10 drop volume tensiometer with different surfactant solutions. A major objective of this work is to develop a procedure for dynamic interfacial tension data interpretation in a drop volume tensiometer that can be applied to both light and dense non-aqueous phase liquids. For this reason, extensive studies were carried out using both experimental configurations A and B, discussed earlier.

5.1 Calibration of the DVT-10 Tensiometer

Typically, interfacial tensions obtained using the drop volume method require correction that depends both on the capillary diameter and the drop volume. Harkin's correction factor, F, is commonly used to correct the experimental data, and is tabulated as a function of the ratio:

$$\delta = r_d / V^{1/3} \qquad [5.1]$$

where V is the volume of the detached drop, and r_d is the radius of the capillary tip. When r_d is extremely small, F is approximately one (Wilkinson, 1972). Since this case applies to the current research, Equation [4.1] is expected to be valid without the need for a correction factor.

In order to establish that this is indeed the case, interfacial tensions were measured between pure organic compounds and deionized water for different syringe pump flow rates. Tables 5.1 and 5.2 give the interfacial tension of dodecane with water, and carbon tetrachloride with water, respectively, for both experimental configurations. In configuration A, the data in Table 5.1 are in good agreement with the literature value of interfacial tension for dodecane / water, which is 52.1 mN/m (Dukhin *et al*, 1995). Thus no correction factor is required. The results also show that the interfacial tension between pure organic compounds and deionized water without surfactants present is independent of the flow rate, as expected. The slight decrease evident in interfacial tension between dodecane and water is likely due to impurities present in the dodecane. However, in configuration B, when deionized water is introduced through the syringe pump, the experimental data for dodecane are in the range of 58.5 to 59.5 mN/m, which is consistently higher than the results obtained in configuration A. This phenomenon is investigated in greater detail in a subsequent section.

For carbon tetrachloride, on the other hand, the experimental data in Table 5.2 obtained from configuration B are in good agreement with the literature value, which is 45.0 mN/m (Adamson, 1990). In configuration A, the interfacial tension data obtained for carbon tetrachloride are around 52 mN/m, which again demonstrates that when water is introduced through the syringe pump, the interfacial tensions are consistently higher. During experiments when water is introduced through the syringe pump, there is a clearly visible neck formed just before the water drop detaches. Figure 5.1 shows a

Table 5.1

Interfacial Tension of Dodecane and Deionized Water

Flow Rate (mL/h)	**Configuration A** γ (mN/m)	**Configuration B** γ (mN/m)
1.00	52.42	59.84
0.75	52.21	59.52
0.50	51.96	59.50
0.25	51.52	59.02
0.10	50.67	58.28

Table 5.2

Interfacial Tension of Carbon Tetrachloride and Deionized Water

Flow Rate (mL/h)	**Configuration A γ (mN/m)**	**Configuration B γ (mN/m)**
1.00	51.98	44.89
0.75	52.01	45.03
0.50	52.22	45.60
0.25	52.04	45.29
0.10	51.64	44.06

typical neck formation in a water drop suspended in mineral oil. When the neck formation occurs, Equation [4.1] is no longer valid. For experiments with dodecane, which is a representative light NAPL, neck formation occurs when water is introduced in configuration B. For experiments with carbon tetrachloride, a representative dense NAPL, neck formation occurs when water is introduced in configuration A. The experimental results thus indicate that when an oil phase is introduced, Equation [4.1] is valid, and because of the small capillary diameter used, no correction factor is needed for the calculation of interfacial tension. When the water phase is introduced, however, Equation [4.1] is no longer valid due to neck formation in the water drop.

Table 5.3 shows the interfacial tensions for mineral oil and water over the range of syringe pump flow rates tested. Tensiometer configuration B again yields consistently higher drop volumes than configuration A due to neck formation in the water drop. The difference in volume is constant over the range of flow rates tested, and has an average value of 6.09 μL. As a consequence, the average value of interfacial tension calculated with configuration B is 9.62 mN/m higher than the average value obtained with configuration A. No dynamic effect of interfacial tension is noted with either configuration.

Neck formation in water drops has a significant effect on dynamic interfacial tension when surfactants are present. Figures 5.2 and 5.3 show dynamic interfacial tensions

Figure 5.1 Typical neck formation in a water drop suspended in mineral oil

Table 5.3

Interfacial Tension of Mineral Oil and Deionized Water

	Configuration A Data		Configuration B Data	
Pump flowrate, mL/h	**Drop volume, μL**	**γ from Eq. [4.1], mN/m**	**Drop volume, μL**	**γ from Eq. [4.1], mN/m**
1.00	28.43	47.66	34.48	57.25
0.75	28.47	47.71	34.48	57.25
0.50	28.47	47.71	34.69	57.58
0.25	28.38	47.60	34.48	57.24
0.10	28.58	47.90	34.67	57.35

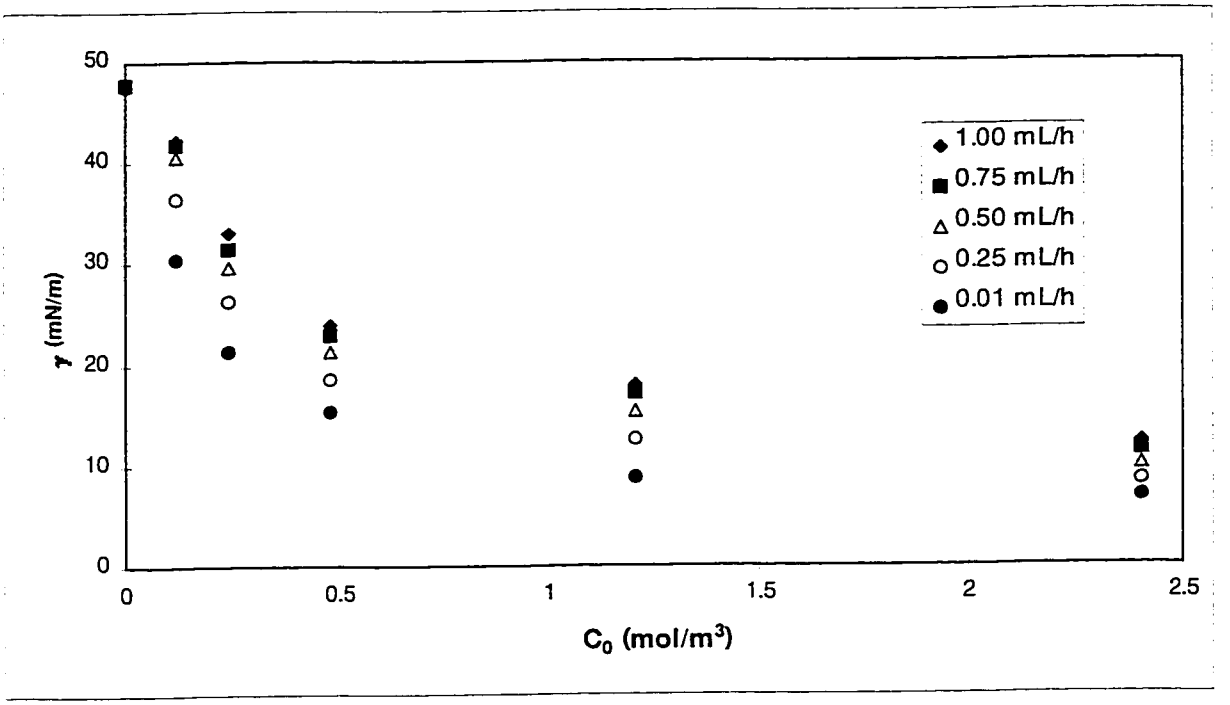

Figure 5.2 Dynamic interfacial tension for Span 80 system in configuration A for the indicated syringe pump flow rate

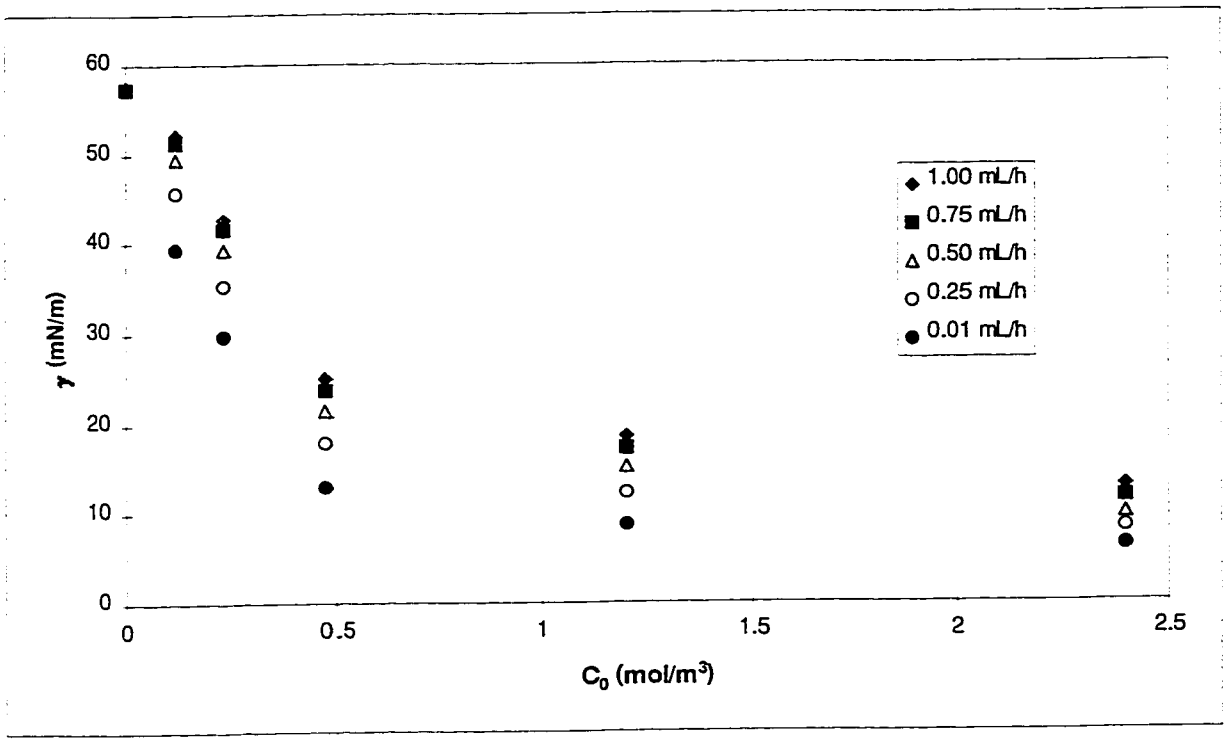

Figure 5.3 Dynamic interfacial tension for Span 80 system in configuration B for the indicated syringe pump flow rate

measured with configuration A and configuration B, respectively, for Span 80 / mineral oil solutions and water. As expected, the interfacial tension decreases with increasing concentration of Span 80, as well as with increasing drop formation time. From the data presented in Figure 5.2, it is possible to calculate cmc of about 1.2 mol/m^3 for Span 80. Figures 5.4 and 5.5 present dynamic interfacial tensions measured with configuration A and configuration B, respectively, for SDS / water solutions and mineral oil. The same trend can be found as with Span 80. As SDS concentration or drop formation time increases for both configurations, the interfacial tension decreases. All concentrations of SDS tested in this research work are well below the cmc of 6.94 mol/m^3 (Bonfillon *et al*, 1994).

For both surfactants tested, the effect of tensiometer configuration on the dynamic interfacial tension is found to be similar. The type of behavior observed is dependent upon surfactant concentration, and upon the absolute value of the dynamic interfacial tension. When surfactant concentration is low relative to the cmc, the dynamic interfacial tension curves obtained with configuration A and configuration B are as shown in Figure 5.6 for 0.012 mol/m^3 Span 80, and in Figure 5.7 for 0.087 mol/m^3 SDS. In each case, the values of dynamic interfacial tension obtained with configuration B are consistently higher for any given drop formation time. For both surfactants, the dynamic interfacial tension curves for the two experimental configurations have the same general appearance, noted in Figure 5.6 and 5.7 above, for a wide range of concentrations. However, once the interfacial tension drops to a value of about 18 mN/m or lower, the interfacial tension

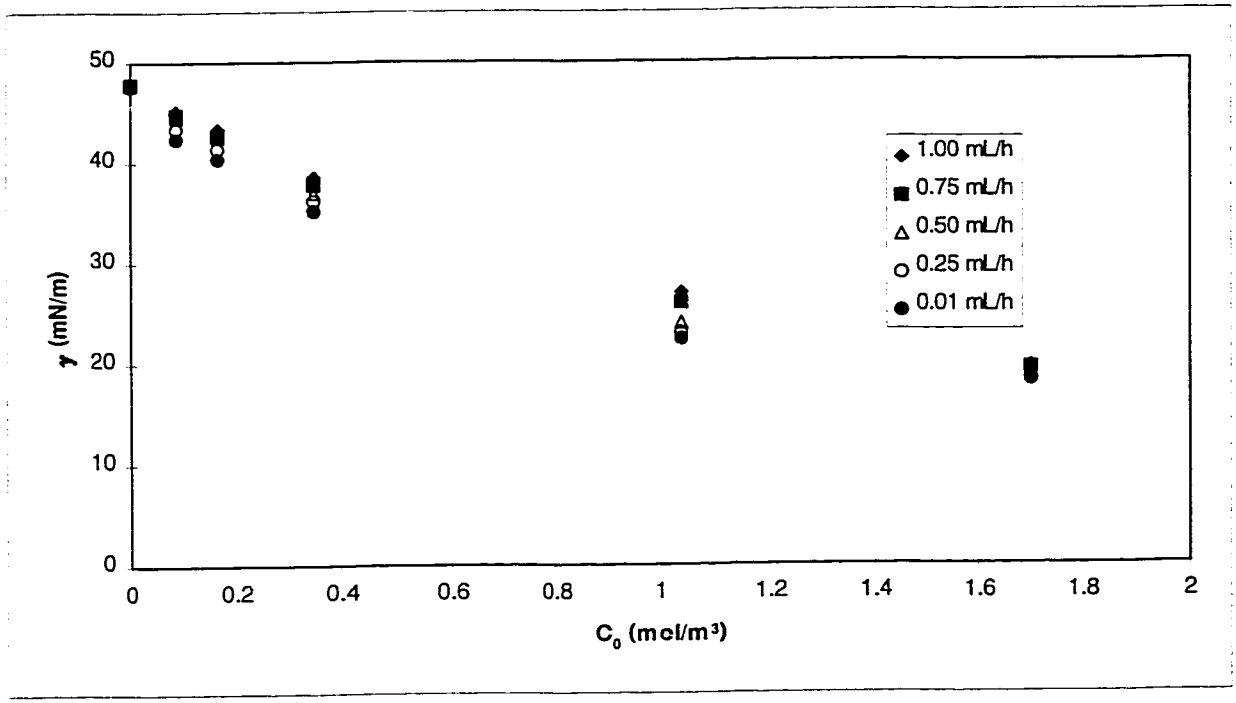

Figure 5.4 Dynamic interfacial tension for SDS system in configuration A for the indicated syringe pump flow rate

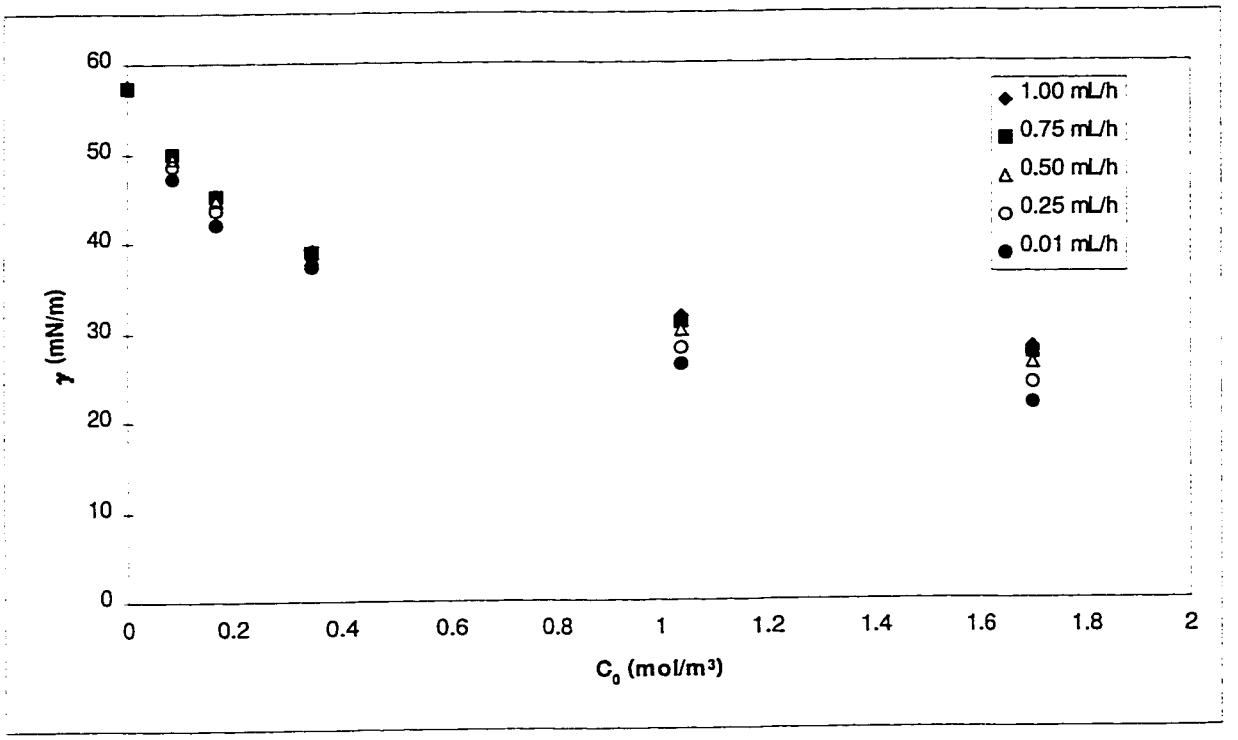

Figure 5.5 Dynamic interfacial tension for SDS system in configuration B for the indicated syringe pump flow rate

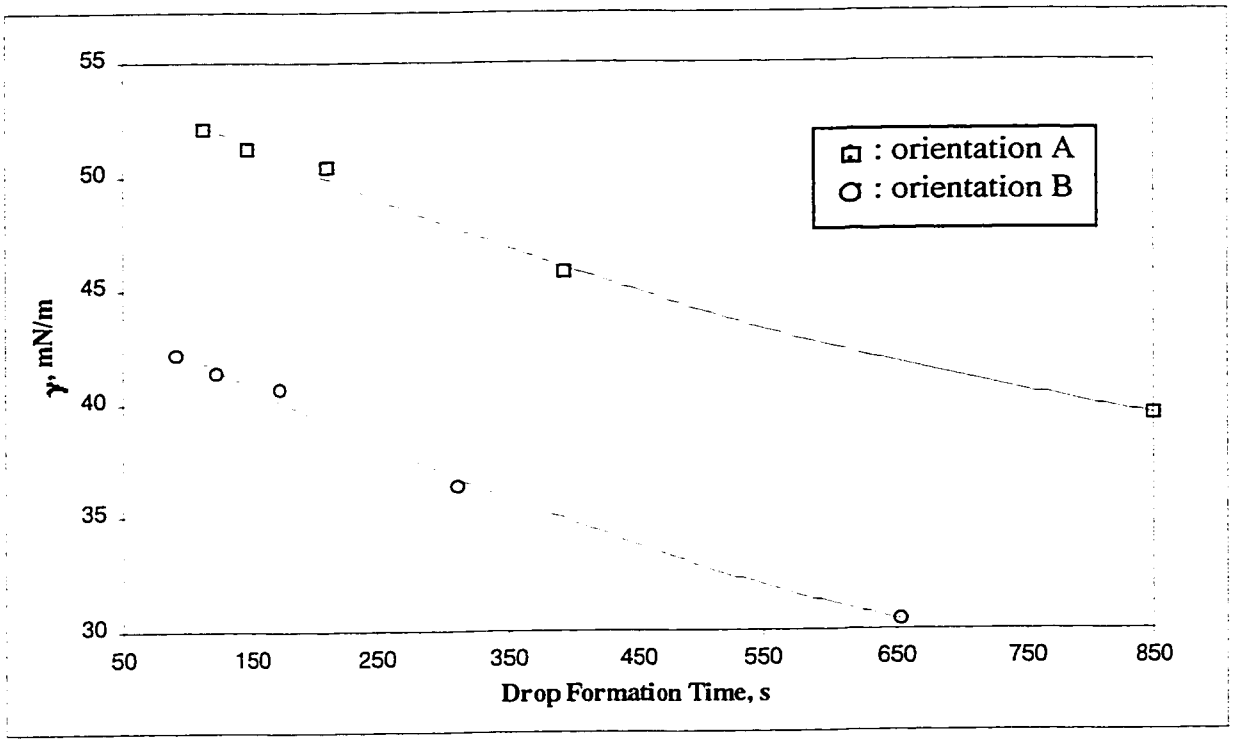

Figure 5.6 Dynamic interfacial tension and capillary orientation for 0.12 mol/m^3 Span 80

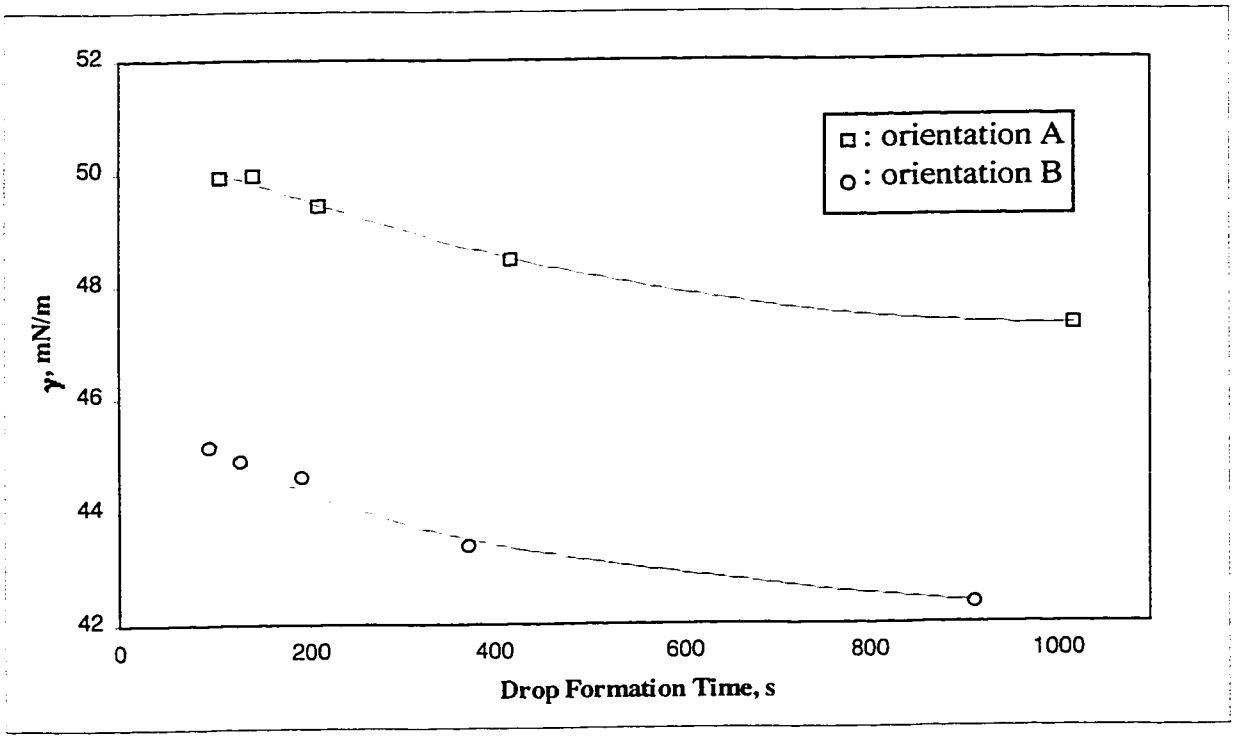

Figure 5.7 Dynamic interfacial tension and capillary orientation for 0.087 mol/m^3 SDS

becomes independent of experimental configuration. When the interfacial tension is 18 mN/m, the corresponding drop volume is about 11 μL. Water drops of this size or less appear to be sufficiently small that neck formation does not occur.

5.2 Modeling the Effect of Neck Formation on Dynamic Interfacial Tension

Since the interfacial tensions of the pure mineral oil-water interface shown in Table 5.3 are independent of flow rate, it can be concluded that hydrodynamic effects on drop formation can be neglected for the flow rates tested. As the experimental data have shown, when a neck is present, the force balance around a detaching drop given in Equation [4.1] is no longer valid. For the case of a slowly growing drop suspended in a vacuum, a force balance at the moment of detachment has been given by Garandet *et al.* (1994) By assuming the drop is axisymmetrical, the forces acting on the pendant drop shown in Figure 5.8 are: its weight, mg, directed downward; the pressure P_n acting on the disc of radius r_n at level z_n, also directed downward; and the surface tension contribution, directed upward.

The resulting force balance at detachment is:

$$\gamma \pi d_n = \varrho_H V_n g + P_n \frac{\pi d_n^2}{4} \qquad [5.2]$$

with d_n being the neck diameter at the moment of detachment, V_n being the volume of the

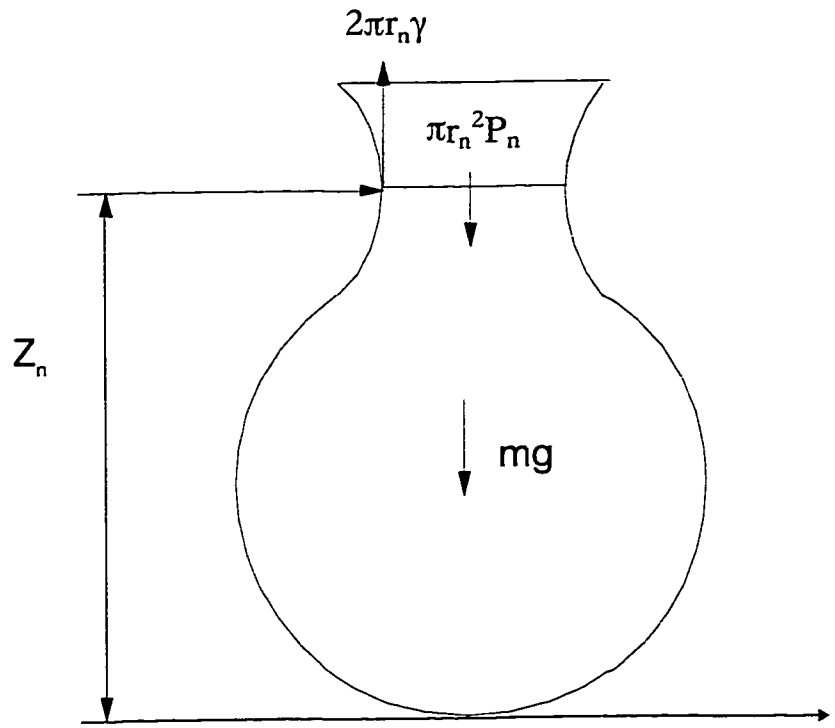

Figure 5.8 Forces acting on a pendant drop

drop including the neck, and P_n being the net pressure acting on the neck at the moment of detachment. P_n consists of two components: the excess pressure ΔP, and the hydrostatic pressure, P_h.

Equation [5.2] neglects the buoyancy force, which must be included in the case under consideration in this work. Thus, for a drop suspended in a liquid in experimental configuration B, the force balance at the moment of detachment becomes:

$$\gamma \pi d_n + \varrho_L V_n g = \varrho_H V_n g + \frac{\pi d_n^2}{4}(\Delta P - P_h) \qquad [5.3]$$

The excess pressure term is frequently described by Laplace's equation, $\Delta P = 2\gamma/b$, where b is the radius of curvature at the bottom of the suspended drop. The hydrostatic pressure acting on the neck is given by $\varrho_L gh$, where h is the immersion depth of the drop neck. Substituting for ΔP and P_h in Equation [5.3], dividing through by πd, and rearranging gives:

$$\frac{(\varrho_H - \varrho_L)V_n g}{\pi d} = \frac{d_n}{d}\gamma - \frac{d_n^2}{4d}\left(\frac{2\gamma}{b} - \varrho_L gh\right) \qquad [5.4]$$

By comparison with Equation [4.1], it can be seen that the term on the left hand side of Equation [5.4] is an apparent interfacial tension based on V_n. Replacing this term by γ_{app}, and combining like terms gives a relationship between γ_{app} and γ :

$$\gamma_{app} = \left(\frac{d_n}{d} - \frac{d_n^2}{2bd}\right)\gamma + \frac{d_n^2 \varrho_L gh}{4d} \qquad [5.5]$$

Equation [5.5] may be used to obtain corrected values of interfacial tension from apparent ones if d_n, b and h are known. However, these parameters are difficult to determine experimentally (Garandet *et al*, 1994). Still it is useful to study the conditions under which Equation [5.5] can be easily applied to dynamic interfacial tension data obtained from drops exhibiting neck formation. Based on the recorded experiments with low concentrations of Span 80, it is possible to make a number of simplifying assumptions. Firstly, it is noted that d_n is approximately equal to d from the videotaped experiments. Secondly, the hydrostatic pressure term can be assumed constant since the depth of immersion of the capillary was not varied for the experiments in configuration B. Equation [5.5] can thus be simplified to give:

$$\gamma_{app} = \left(1 - \frac{d}{2b}\right)\gamma + k_h \qquad [5.6]$$

where k_h is a constant term related to hydrostatic pressure. If the parameter b can be assumed to remain constant over a given interval of drop formation times and surfactant concentrations, then Equation [5.6] presents a linear relationship between apparent and actual interfacial tensions (Campanelli and Wang, 1997A).

For the special case of a small, spherical drop (i.e. with no neck), the hydrostatic pressure term can be dropped, and d_n can be replaced by d in Equation [5.6] to give:

$$\gamma_{app} = \left(1 - \frac{d}{2b}\right)\gamma \qquad [5.7]$$

which is the same result obtained by Garandet *et al.* (1994) In the present study, d is 0.254 mm, while 2b is on the order of several millimeters. Thus, d << 2b, and Equation [5.7] can be approximated by $\gamma_{app} = \gamma$. This relationship explains why the interfacial tension of drops with no visible necking is independent of experimental configuration.

The usefulness of Equation [5.6] in correlating the dynamic interfacial tension data for low concentrations of Span 80 is shown in Figure 5.9. Data pairs of γ and γ_{app} are chosen for the same drop formation times from experimental curves, such as the one shown in Figure 5.6. In Figure 5.9, the data for concentrations of 0.12 mol/m^3 and 0.24 mol/m^3 of Span 80 fall on the same line. Regression analysis gives an excellent correlation, with a slope of 0.96, and an intercept of 12.1 mN/m. From the slope, a value of 3.1 mm can be calculated for the parameter b. The immersion depth can be calculated from the value of the intercept to be about 2.2 cm. Both of these values appear to be reasonable when compared to observations from the videotaped experiments. Thus, Equation [5.6] represents a useful model for the determination of actual values of dynamic interfacial tensions from apparent ones at Span 80 concentrations below the cmc.

Figure 5.10 shows that Equation [5.6] cannot, however, be generalized to all types of surfactants. The figure plots γ_{app} versus γ for SDS concentrations ranging from 0.043 mol/m^3 to 0.35 mol/m^3. It can be seen that the SDS data lie below the dotted line which represents the solution of Equation [5.6] for Span 80. The assumption that $d_n = d$ does not

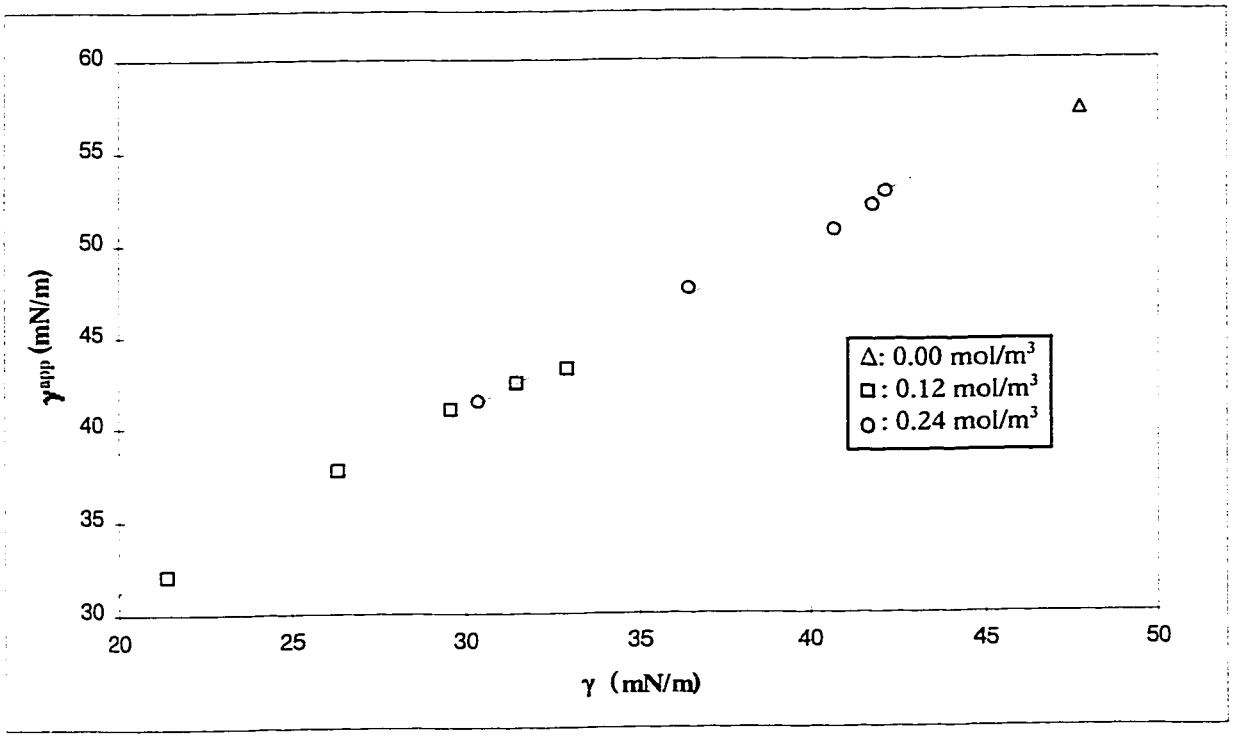

Figure 5.9 Solution of Eq. [5.6] for Span 80 data

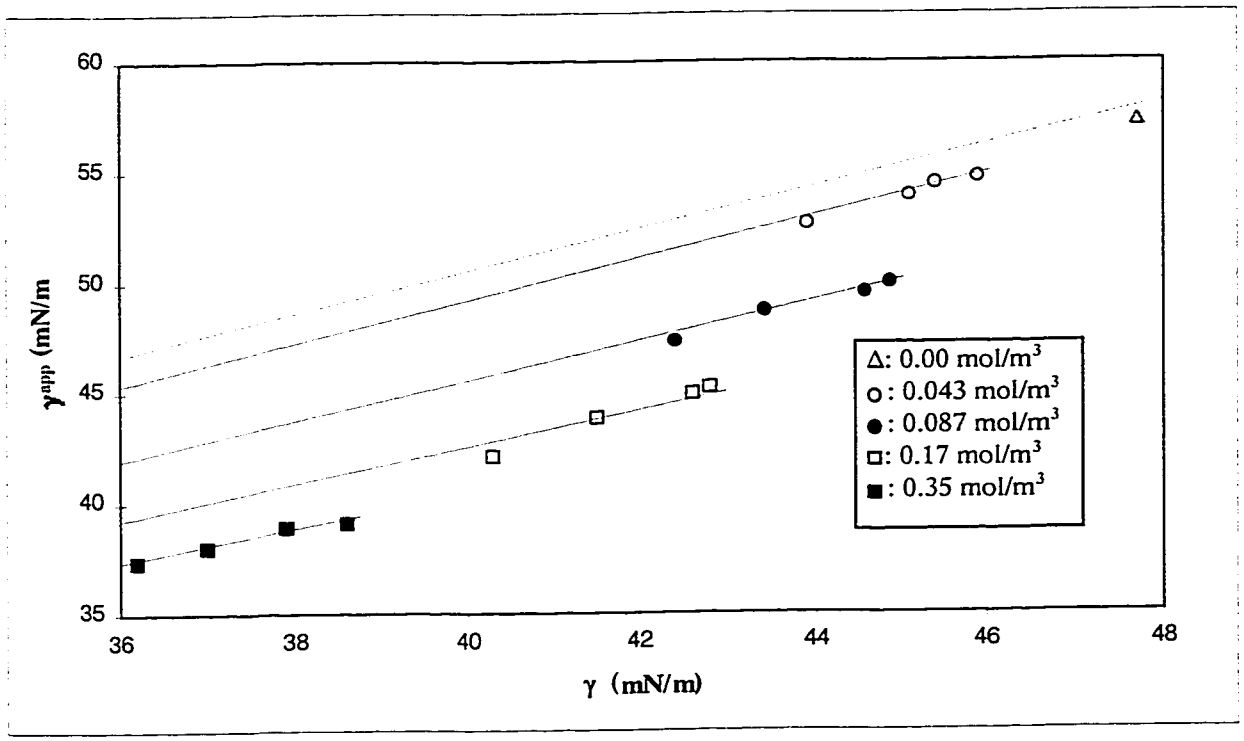

Figure 5.10 Solution of Eq. [5.5] for SDS data

appear to be a valid one for the SDS data. The videotaped experiments indicate that d_n may in fact be slightly smaller than d. It was not possible to obtain a precise determination of d_n with the available equipment. However, a theoretical analysis based on Equation [5.5] is still possible.

The solids lines drawn through the data sets in Figure 5.10 represent solutions to Equation [5.5] using various values of d_n/d, and using the values for h and b that were determined from the Span 80 experiments. When d_n/d is assumed to remain constant at a value of 0.99, the solution to Equation [5.5] is a line which agrees well with the data for an SDS concentration of 0.043 mol/m^3. In a similar fashion, d_n/d values of 0.94, 0.88, and 0.84 provide reasonable fits of Equation [5.5] with SDS concentrations of 0.087 mol/m^3, 0.17 mol/m^3 and 0.35 mol/m^3, respectively. Concentrations exceeding 0.35 mol/m^3 did not yield linear plots of γ_{app} versus γ. This finding may result from the build-up of interfacial charge, which presents a barrier to surfactant adsorption at higher SDS concentrations (Bonfillon *et al*, 1994). It can therefore be concluded that Equation [5.5] represents a valid model for interpreting dynamic interfacial tension data when necking occurs in the suspended drop.

Chapter 6. Models for Surfactant Adsorption Processes

The procedure developed for experimental determination of dynamic interfacial tension, and for data analysis, is used in this section to model adsorption of surfactants at the mineral oil / water interface.

6.1 Experimental Results for Selected Surfactants

By controlling the flow rate of the DVT-10 syringe pump, the dynamic interfacial tensions for the selected surfactants can be measured at different surfactant concentrations. These results are presented below.

Figure 6.1 shows dynamic interfacial tension data for Triton X-100 at the mineral oil / water interface. These data, along with the data shown in Figure 5.2 for Span 80, and in Figure 5.4 for SDS, are not well-suited to the study of adsorption kinetics. Plots of dynamic interfacial tension versus drop formation time are required. These plots are shown in Figures 6.2, 6.3 and 6.4 for Span 80, SDS and Triton X-100, respectively, at the mineral oil / water interface. It can be noted from the variations in interfacial tension with drop formation time that dynamic effects are more pronounced for Span 80 and Triton X-100 than for SDS.

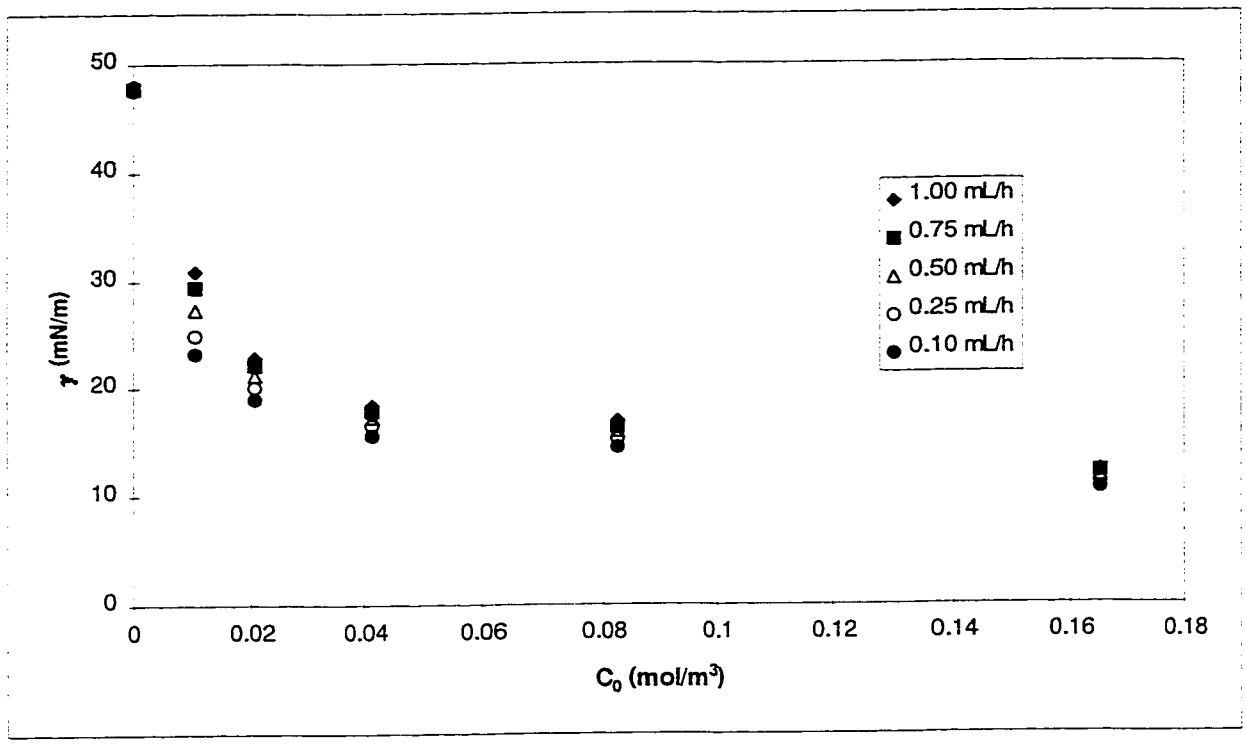

Figure 6.1 Dynamic interfacial tension for Triton X-100 system in configuration A for the indicated syringe pump flow rates

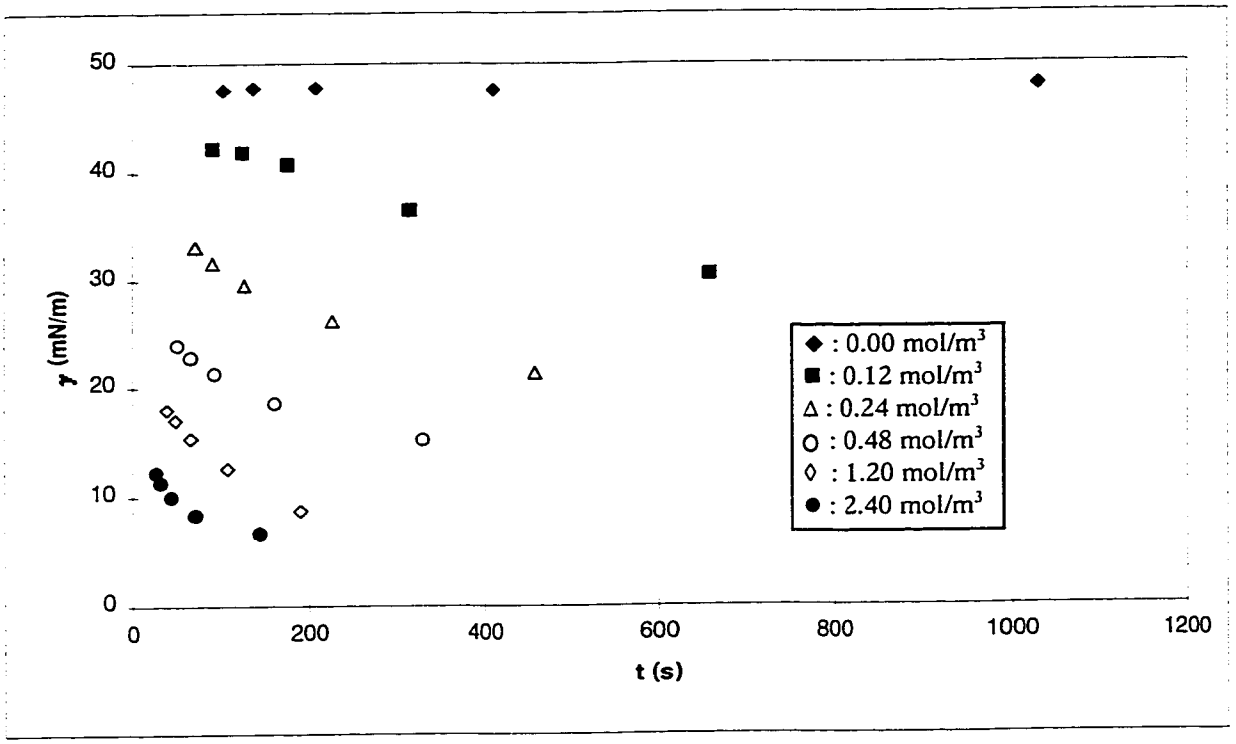

Figure 6.2 Dynamic interfacial tension versus drop formation time for Span 80

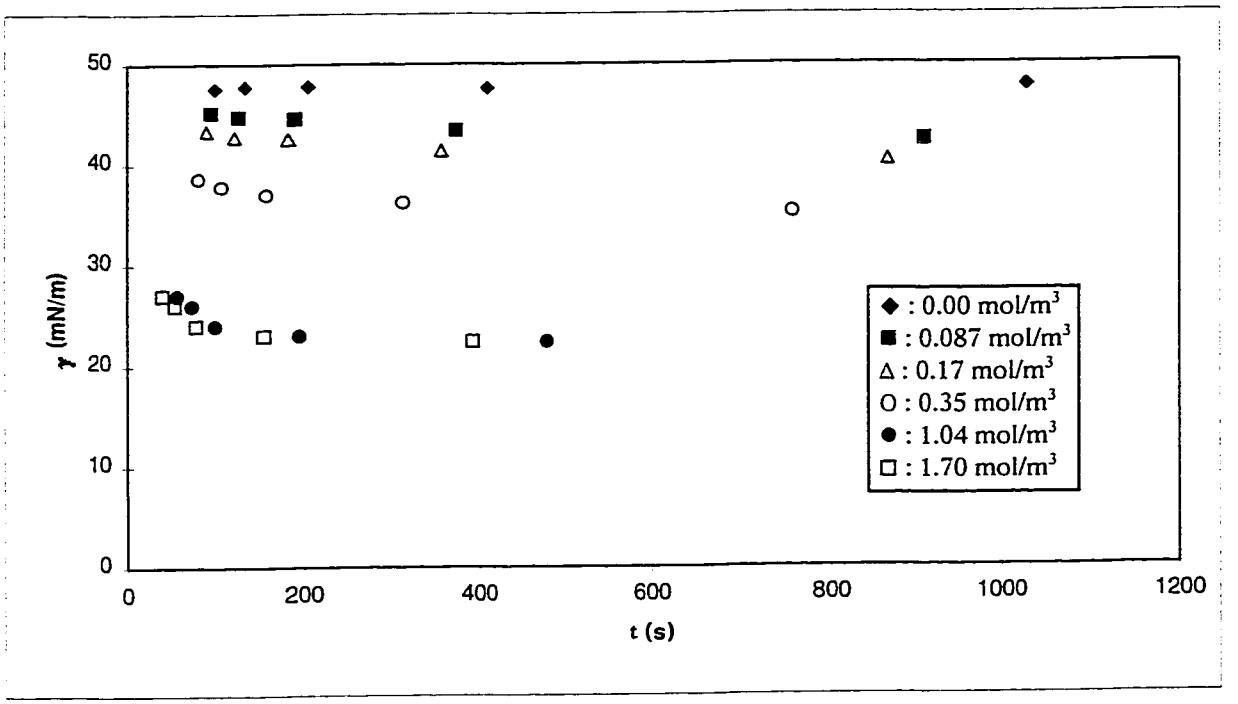

Figure 6.3 Dynamic interfacial tension versus drop formation time for SDS

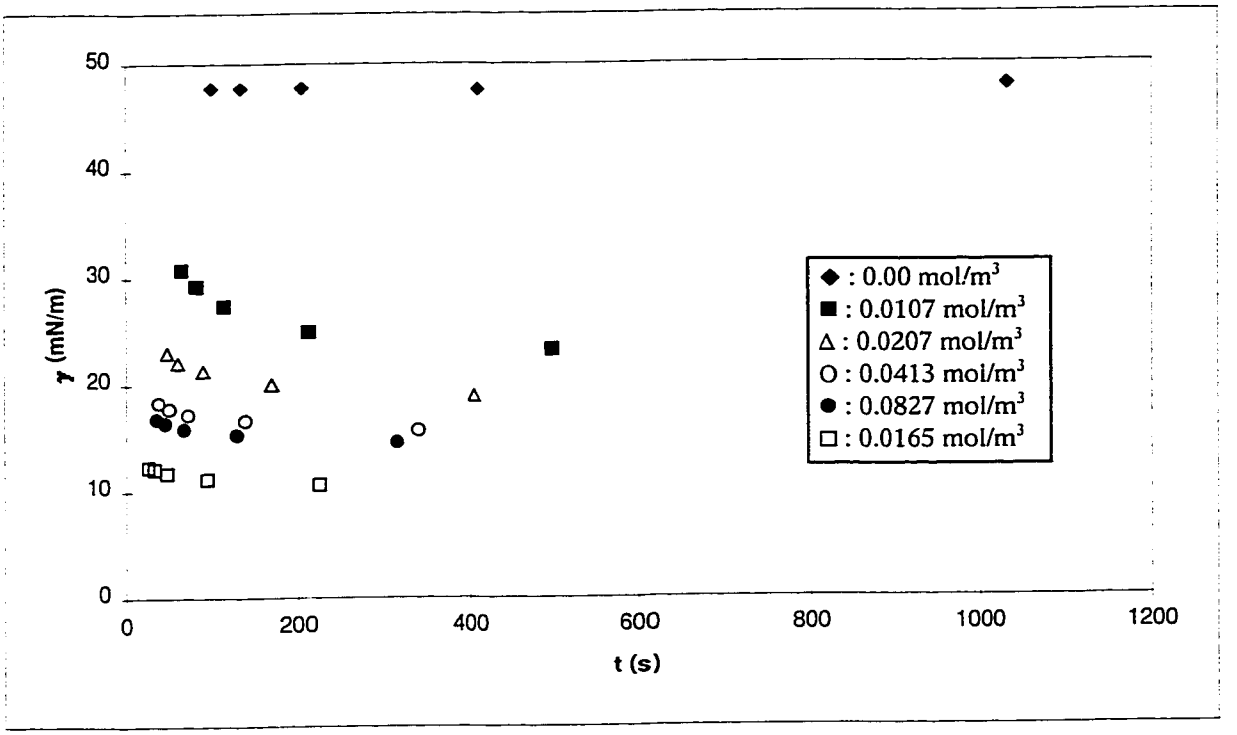

Figure 6.4 Dynamic interfacial tension versus drop formation time for Triton X-100

By testing the fit of the experimental results with the various adsorption models presented in Chapter 2, it is possible to determine that the SDS data are consistent with a kinetic-controlled model, while the Span 80 and Triton X-100 data are consistent with diffusion-controlled models. These models are evaluated in the following sections.

6.2 Kinetic Controlled Model for SDS

Kinetic-controlled adsorption at the liquid-liquid interface includes both adsorption and desorption processes. Desorption can be neglected when the surfactant concentration is small, or at the beginning of the adsorption process. Under these conditions, Equation [2.16] can be simplified to give:

$$\frac{d\Gamma}{dt} = k_{ad} C_0 \left(1 - \frac{\Gamma}{\Gamma_\infty}\right) \qquad [6.1]$$

The Henry isotherm is usually valid under these same adsorption conditions:

$$\gamma = \gamma_0 - RT\Gamma \qquad [6.2]$$

Substituting Equation [6.2] into Equation [6.1] gives, finally (Wang and Campanelli, 1997):

$$\ln\left[\frac{\gamma(t) - \gamma_e}{\gamma_0 - \gamma_e}\right] = -\frac{k_{ad} C_0}{\Gamma_\infty} t \qquad [6.3]$$

Thus, a plot of $\ln\left[\frac{\gamma(t)-\gamma_e}{\gamma_0-\gamma_e}\right]$ vs. t will yield a straight line with a slope equal to $-k_{ad}C_0/\Gamma_\infty$ for kinetic-controlled adsorption. Figure 6.5 shows the plot of $\ln\left[\frac{\gamma-\gamma_e}{\gamma_0-\gamma_e}\right]$ as a function of drop formation time for different SDS concentrations. Since the concentrations tested are well below cmc, the desorption process can be neglected, and the kinetic-controlled adsorption model provides a good fit to the SDS experimental data. The adsorption rate constant is found to be in the range of 0.14×10^{-4} to 0.37×10^{-4} cm/s, in the concentration range tested.

According to Bonfillon *et al* (1994), for drop formation times smaller than 10s, SDS adsorption is diffusion-controlled. However, in this work, the drop formation time is much longer than 10s. As drop formation time increases, the adsorbed surfactant ions produce an increasing electrostatic potential at the interface, which creates a potential barrier and slows the adsorption of new surfactant ions. The drop formation times that are studied in this work are in the range where the electrostatic potential cannot be neglected. This potential barrier controls the adsorption process, and results in a kinetically-controlled adsorption rate, that appears to be independent of the surfactant concentration in the range under consideration.

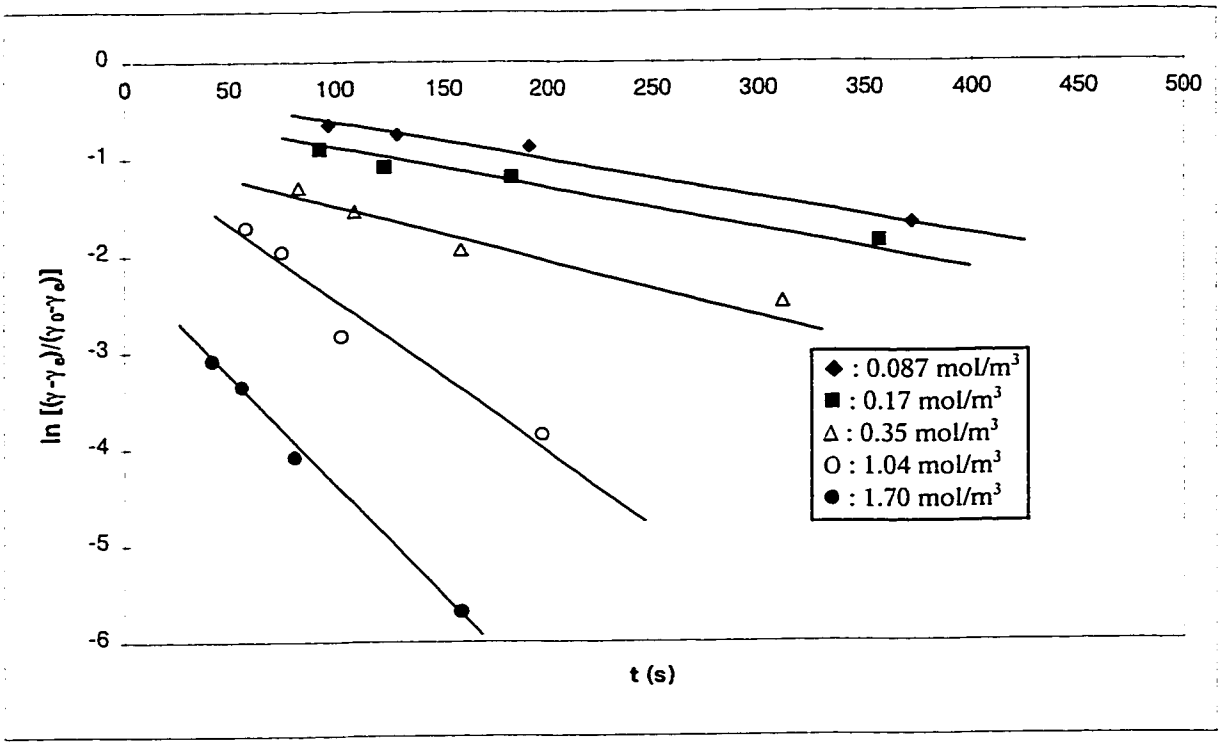

Figure 6.5 Kinetic-controlled model for SDS data

6.3 Diffusion Controlled Model for Span 80

Adsorption is consistent with the short-time approximation of the diffusion-controlled model if a plot of interfacial tension vs. square root of drop formation time yields a straight line according to Equation [2.10]. Figure 6.6 represents such a plot for the Span 80 data. Linear regression for the different Span 80 concentrations gives correlation coefficients, r^2, of 0.984 to 0.997, indicating excellent agreement with Equation [2.10]. The only exception is the Span 80 concentration of 2.4 mol/m^3, which is far above the cmc. When the surfactant concentration is above the cmc, the presence of micelles in the bulk phase can not be ignored. Surfactant monomers can either form micelles or diffuse to the interface. Thus, any diffusion-controlled model based solely on the measurement of interfacial tension will no longer be valid. Micellar kinetics must also be considered.

Diffusion coefficients can be calculated from the slopes of the lines in Figure 6.6, and are listed in Table 6.1. The calculated diffusion coefficients are one or two orders of magnitude smaller than the expected range for aqueous systems because Span 80 is dissolved in the oil phase. According to Wilke and Chang (1955), the diffusion coefficient is inversely proportional to the viscosity of the solvent:

$$D = \frac{9.96 \times 10^{-16} T}{\mu v^{1/3}} \qquad [6.4]$$

where μ is the viscosity of the solution, and v is the solute molar volume. Since the viscosity of mineral oil is 22.7 mPa s, the diffusion coefficients for Span 80 in mineral oil

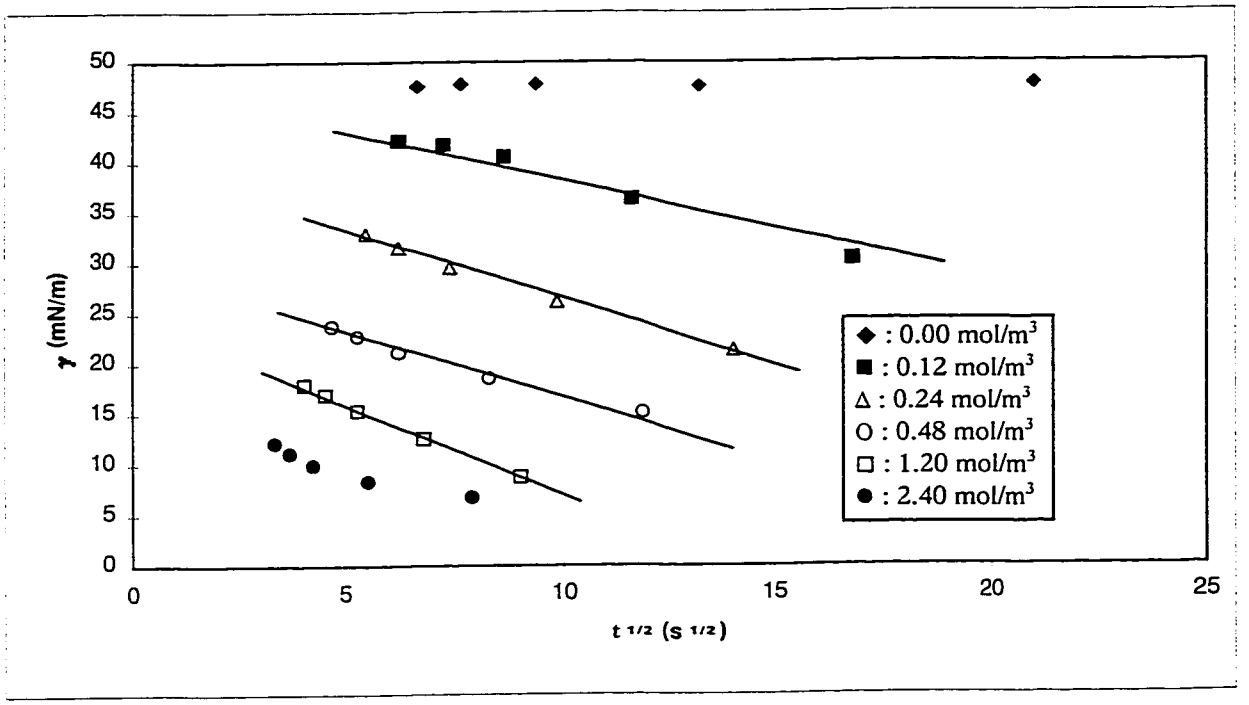

Figure 6.6 Diffusion-controlled model for Span 80 data

Table 6.1

Calculated Values of Diffusion Coefficient for Span 80

Surfactant Concentration (mol/m^3)	**r^2 from Linear Regression**	**Diffusion Coefficient** (m^2/s)
0.12	0.991	2.8×10^{-11}
0.24	0.992	1.0×10^{-11}
0.48	0.984	0.2×10^{-11}
1.20	0.997	0.1×10^{-11}

are thus one to two orders of magnitude smaller than typical aqueous values of diffusion coefficient. These results indicate that Span 80 is a slow diffusing surfactant due primarily to the viscosity of the mineral oil. From Table 6.1, the diffusion coefficients are seen to decrease with increasing surfactant concentration. This phenomenon is attributed to increasing micelle concentrations in the bulk. The presence of micelles decreases the overall diffusion of surfactant to the interface. This agreement with a diffusion-controlled adsorption model for Span 80 is contrary to the findings of Van Hunsel *et al.* (1986), who postulated that surfactants dissolved in an oil phase generally exhibit first order adsorption kinetics.

6.4 Diffusion Controlled Model for Triton X-100

Triton X-100 is found to fit the long-time approximation of diffusion controlled adsorption. Figure 6.7 shows the data for Triton X-100 plotted as a function of $t^{-1/2}$. The resultant linearity of the data indicates that the agreement with Equation [2.13] is quite good. From the slopes of the lines, it is possible to calculate diffusion coefficients for each concentration, and these are presented in Table 6.2. The value of D is of the expected order of magnitude. Since Triton X-100 is dissolved in water, the values of D are much greater than the values for Span 80 in Table 6.1. The trend of a decrease in the value of the diffusion coefficient with an increase in surfactant concentration above 0.0207 mol/m^3 has also been observed by other researchers (Van Hunsel *et al.*, 1986), and has been attributed to the partitioning of surfactant monomer between the interface and a growing number of micelles in the bulk (Rosen and Song, 1996). The magnitude of the

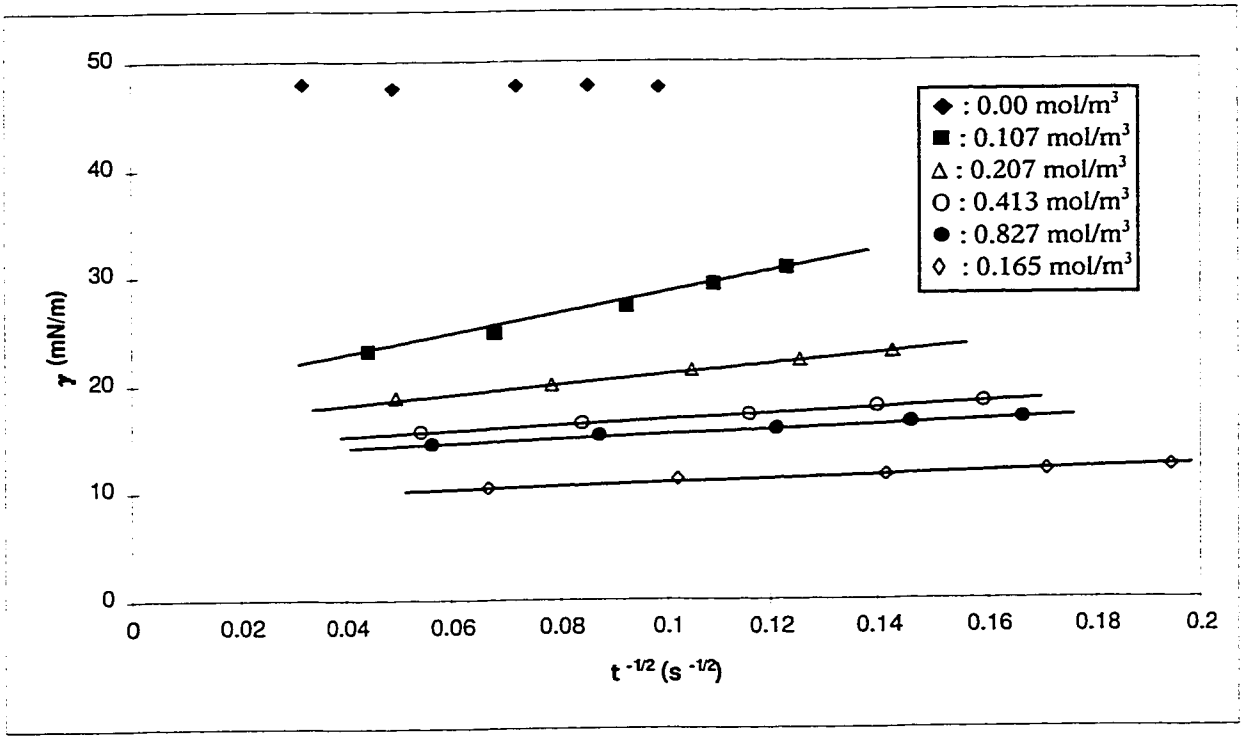

Figure 6.7 Diffusion controlled model for Triton X-100 data

Table 6.2

Calculated Values of Diffusion Coefficient for Triton X-100

Surfactant Concentration (mol/m^3)	**r^2 from Linear Regression**	**Diffusion Coefficient** (m^2/s)
0.0107	0.991	4.06×10^{-10}
0.0207	0.999	6.88×10^{-10}
0.0413	0.999	5.48×10^{-10}
0.0827	0.996	2.24×10^{-10}
0.165	0.997	2.02×10^{-10}

decrease exhibited in the present work is, however, somewhat larger than the decrease reported in Van Hunsel *et al.* (1986)

6.5 General Conclusions for Diffusion Controlled Models

In order to analyze diffusion-controlled surfactant adsorption, it is very useful to be able to determine whether the adsorption process is in the initial stage, or near equilibrium. In the former case, Equation [2.10] should be valid; in the latter case, Equation [2.13] applies.

As discussed in Chapter 2, the ratio of adsorption time, t_a, to τ_D should be an important parameter in modeling the diffusion-controlled adsorption of surfactants. In this ratio, t_a is obtained from t through the application of Equation [2.3]. The characteristic surfactant diffusion time, τ_D, as defined in Equation [2.14], is seem to be a function of the square of the term $d\Gamma/dC_o$. It is thus important to select a valid equation of state in order to avoid introducing large errors into the determination of τ_D. (Campanelli and Wang, 1997B).

For all the plots of interfacial tension versus drop formation time, the interfacial tension decreases to a limiting value, γ_e, as drop formation time increases. The interfacial concentrations at equilibrium, Γ_e, can be obtained from the values of γ_e for each bulk surfactant concentration through the application of the Gibbs Equation, Equation [2.3]. These results are presented in Table 6.3 for Span 80, and in Table 6.4 for Triton X-100.

Table 6.3

Equilibrium Interfacial Concentrations of Span 80 Calculated from the Gibbs Equation

C_0 (mol/m^3)	γ_e (mN/m)	Γ_e (mol/m^2)
0.12	24.5	3.81×10^{-6}
0.24	15.0	3.81×10^{-6}
0.48	10.0	3.81×10^{-6}
1.20	2.50	3.81×10^{-6}

Table 6.4

Equilibrium Interfacial Concentrations

of Triton X-100 Calculated from the Gibbs Equation

C_0 (mol/m^3)	γ_e (mN/m)	Γ_e (mol/m^2)
0.0107	23.0	2.05×10^{-6}
0.0207	19.2	2.16×10^{-6}
0.0413	15.5	2.18×10^{-6}
0.0827	13.0	2.24×10^{-6}
0.165	9.5	2.50×10^{-6}

For Triton X-100, the Langmuir isotherm is valid for concentrations below the cmc (Horozov and Joos, 1995; Rillaerts and Joos, 1982). The Langmuir isotherm can be written as:

$$\Gamma = \Gamma_{\infty}\left(\frac{C_o}{a_L + C_o}\right) \qquad [6.5]$$

where a_L is a constant to be determined experimentally. Differentiating with respect to concentration and substituting into Equation [2.14], gives the following expression for τ_D:

$$\tau_D = \frac{1}{D}\left[\frac{\Gamma_{\infty} a_L}{(a_L + C_o)^2}\right]^2 \qquad [6.6]$$

Figure 6.8 shows the fit of the Langmuir isotherm to the data for Triton X-100. The curve yields values of $\Gamma_{\infty} = 2.43 \times 10^{-6}$ mol/m^3, and $a_L = 2.38 \times 10^{-3}$ mol/m^3, in good agreement with the literature (Horozov and Joos, 1995).

To get the value of τ_D, values of diffusion coefficients are needed. Before actually applying any adsorption model to the experimental data, the diffusion coefficient is not known accurately. For aqueous surfactants an approximate value for D of 10^{-10} m^2/s, which is of the right order of magnitude, can be used. For the concentration range from 0.0107 mol/m^3 to 0.0827 mol/m^3 of Triton X-100, the corresponding range of τ_D is from 11 s to 0.0064 s. The drop formation time in the experiments was varied from about 40 s to 500 s. Values of t_a/τ_D can thus vary from about 2 to 33 000. This range of magnitudes

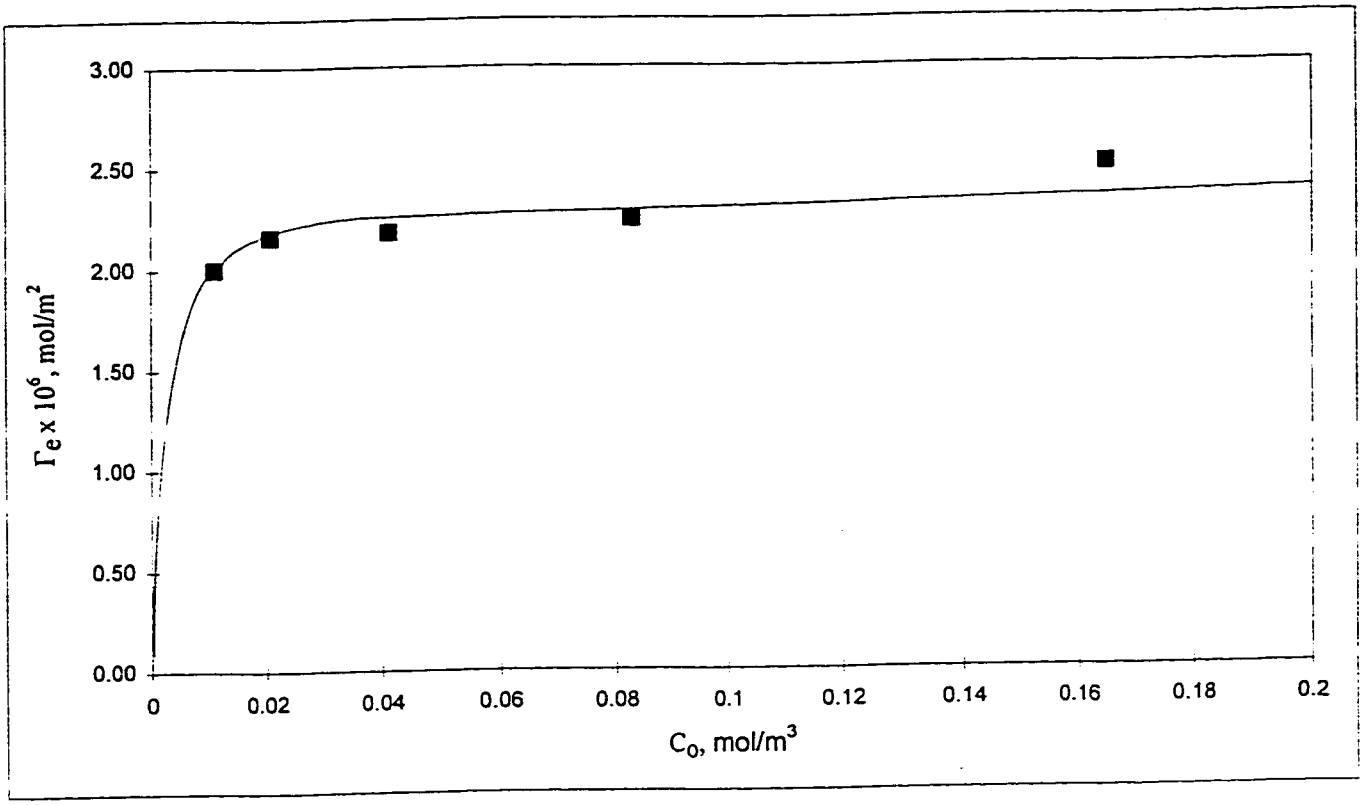

Figure 6.8 Langmuir isotherm for Triton X-100 data

indicates that the adsorption time is much greater than the characteristic diffusion time of the surfactant, and that the long-time approximation of the diffusion equation should be valid. Figure 6.7 shows that this is indeed the case, as discussed previously.

Using the tabulated values of D that were calculated from the long-time approximation in Table 6.2 for Triton X-100, it is possible to calculate more accurate values of τ_D for each surfactant concentration tested. These values, along with the corresponding range in t_a and the ratio t_a/τ_D, are shown in Table 6.5. In all cases, t_a/τ_D is on the order of 10 or greater. This result demonstrates the usefulness of a rough calculation of t_a/τ_D, and provides justification for the use of the long-time approximation for Triton X-100.

An inspection of the Span 80 data in Table 6.3 reveals that the interfacial concentrations change very little with bulk concentration, and can be considered to be very close to the equilibrium value. For such a case, Joos *et al.* (1992) have proposed a characteristic time for surfactant diffusion based on the equation of Ward and Tordai. After correction of the typographical error in the paper of Joos *et al.*(1992), the equation to obtain the characteristic diffusion time of such a surfactant becomes:

$$\tau_D = \frac{7\pi}{12D}\left(\frac{\Gamma_e}{C_o}\right)^2 \qquad [6.7]$$

From the data for Span 80, $\Gamma_e = 3.81 \times 10^{-6}$ mol/m^2. Again, a typical value of diffusion coefficient can be estimated for an approximate determination of τ_D. Since mineral oil is

Table 6.5

Calculated Values of t_a/τ_D for Triton X-100

C_0 (mol/m^3)	D (m^2/s)	τ_D (s)	t_a (s)	t_a/τ_D
0.0107	4.06×10^{-10}	2.8	28 - 210	11 - 77
0.0207	6.88×10^{-10}	0.17	21 - 180	120 - 1000
0.0413	5.48×10^{-10}	0.017	17 - 150	$(1.0 - 8.6) \times 10^3$
0.0827	2.24×10^{-10}	2.9×10^{-3}	15 - 130	$(0.51 - 4.6) \times 10^4$
0.165	2.02×10^{-10}	1.2×10^{-5}	12 - 99	$(1.0 - 8.1) \times 10^6$

the solvent for Span 80, D will be approximately 1/22.7 times the corresponding value in water, due to the effect of solvent viscosity. Therefore, a value for D of 5 x 10^{-12} m^2/s is selected as being of the appropriate order of magnitude. For the concentration range tested in this study, τ_D lies in the range 10 s to 350 s. For drop formation times of 40 s to 650 s, values of t_a/τ_D can vary from about 0.03 to 30. This range is much lower than the range of t_a/τ_D for Triton X-100. The characteristic diffusion time of Span 80 is thus likely to be more important than the adsorption time in the experiments, and the short time approximation should be valid. Figure 6.6 shows that this approximation provides a good fit to the experimental data, as previously discussed.

The values of diffusion coefficients in Table 6.1 are used to calculate more accurate values of τ_D, from which t_a/τ_D values are obtained, as before. The results are shown in Table 6.6. In this case, the values of t_a/τ_D are in the range 0.3 to 5. By considering the results for Triton X-100 and Span 80 together, it may be concluded that values of t_a/τ_D on the order of unity or less are consistent with the short time approximation of diffusion-controlled adsorption. Values of t_a/τ_D on the order of ten or greater indicate that the long time approximation is more suitable for modeling the adsorption dynamics.

The general applicability of this conclusion is tested by considering previously published surfactant diffusion data. Table 6.7 presents an analysis of the data of Van Hunsel *et al.* (1986), and Joos *et al.* (1992). In the former paper, the drop volume method was used to obtain the dynamic interfacial tension data, while the maximum bubble pressure method

Table 6.6

Calculated Values of t_a/τ_D for Span 80

C_0 (mol/m^3)	D (m^2/s)	τ_D (s)	t_a (s)	t_a/τ_D
0.12	2.87×10^{-11}	64	39 - 280	0.61 - 4.4
0.24	9.52×10^{-12}	48	30 - 200	0.62 - 4.2
0.48	1.83×10^{-12}	63	22 - 140	0.35 - 2.2
1.20	0.74×10^{-12}	25	17 - 82	0.68 - 3.3

Table 6.7

Values of t_a/τ_D from the Data of Van Hunsel *et al.* (1986) and of Joos *et al.* (1992)

C_0 (mol/m^3)	D (m^2/s)	τ_D (s)	t_a (s)	t_a/τ_D
Triton X-100 (Van Hunsel *et al.*)				
0.0216	2.3×10^{-10}	0.47	2 - 25	4.3 - 53
0.11	1.9×10^{-10}	0.0012	1.5 - 16	1200 - 14000
Bry 58 (Van Hunsel *et al.*)				
0.01		33	1 - 12	0.03 - 0.36
C_{12}BMG (Joos *et al.*)				
0.078		2.0	0.4 - 43	0.2 - 22
0.15		0.44	0.4 - 43	0.9 - 98
0.20		0.20	0.2 - 43	1 - 220
0.30		0.059	0.2 - 43	3.4 - 730
0.39		0.025	0.04 - 13	1.6 - 520
0.60		0.0058	0.04 - 13	6.9 - 2200
1.02		0.00085	0.04 - 13	47 - 15000
$C_{12}EOSO_4Na$ + 0.1 N NaCl (Joos *et al.*)				
0.30		2	0.4 - 43	0.2 - 22
0.37		1.3	0.6 - 43	0.5 - 33
0.495		0.72	0.3 - 43	0.4 - 60
0.74		0.3	0.3 - 43	1 - 140

was used in the latter work. Van Hunsel *et al.* considered the commercial surfactants Triton X-100 and Bry 58 at the water-hexane interface. Joos *et al.* studied the surfactants C_{12}BMG (n-dodecyl-n-methylglycine), and $C_{12}EOSO_4$ (a sodium salt of sulfated, polyoxyethylated, n-dodecyl alcohol) at the air-water interface.

For the two concentrations of Triton X-100 tested by Van Hunsel *et al.,* Equation [6.6] is used to obtain the tabulated values of τ_D. The values of D that were obtained by these authors using the long time approximation are in reasonable agreement with the results presented in this work, although at the lower concentration the values differ by close to a factor of three. Nevertheless, the calculated values of τ_D for the corresponding approximate concentrations are of the same order of magnitude. The tabulated values of t_a/τ_D are found to be significantly greater than one, as expected. Diffusion coefficient is, therefore, not a parameter to which the ratio t_a/τ_D is particularly sensitive. Rough estimates of D are thus sufficient for the characterization of the adsorption process.

The data for Bry 58 at a concentration of 1×10^{-2} mol/m^3 were shown to fit the short-time approximation for early adsorption times. The authors noted that Γ could be considered constant, so τ_D was calculated using Equation [6.7] with $\Gamma_e = 2.7 \times 10^{-6}$ mol/m^2. The values for t_a/τ_D shown in Table 6.7 are below unity, as expected.

The data for C_{12}BMG were found to provide a good fit with the long-time approximation for a wide range of concentrations. The authors showed that Γ was well-described by a

Langmuir isotherm with Γ_∞ = 4.4 x 10^{-6} mol/m^2, and a_L = 8 x 10^{-2} mol/m^3. Using Equation [6.6], τ_D was calculated for each concentration. Except for the earliest times at the lowest concentration tested (C_o = 0.078 mol/m^3), the values of t_a/τ_D are all above unity.

The data for $C_{12}EOSO_4$ in 0.1 N NaCl solution were also found to fit the long time approximation. In this case, however, the value for Γ did not change considerably over the concentration range tested. Therefore, Equation [6.7] was used with Γ_e = 3.1 x 10^{-6} mol/m^2, and D = 10^{-10} m^2/s. Except for the earliest adsorption times, all values of t_a/τ_D are larger than unity, as expected.

The examination of adsorption data from the experiments reported in this work, as well as from previous research work, illustrates the usefulness of the quantity t_a/τ_D in characterizing diffusion-controlled adsorption. An order of magnitude estimate of the diffusion coefficient appears to be sufficient in order to obtain reliable values of t_a/τ_D. However, the ratio is much more sensitive to the choice of surface equation of state, since τ_D varies with the square of the differential of the selected function.

Chapter 7. Conclusions and Recommendations

The overall objective of this research work is to model the adsorption of selected surfactants at the water / HOCs interface using a drop volume tensiometer. This objective has been met, and the following contributions to knowledge have been made:

- a theoretical basis for interpreting dynamic interfacial tension data which accounts for neck formation has been proposed;
- a kinetic-controlled adsorption model has been shown to be consistent with data for SDS at the mineral oil / water interface;
- two diffusion-controlled adsorption models have been found to be consistent with dynamic interfacial tension data for each of Triton X-100 and Span 80 surfactants at the mineral oil / water interface;
- a dimensionless quantity relating adsorption time to a characteristic time for a given surfactant has been shown to be correlated with the progression of diffusion-controlled adsorption.

These contributions are elaborated more fully below.

A drop volume tensiometer was used to study surfactant adsorption at liquid-liquid interfaces. However, in order to apply the technique to both light and dense NAPLs, it was necessary to develop a method to account for neck formation in suspended drops.

A model first proposed for the calculation of the surface tension of a slowly-growing, suspended drop has been modified to interpret dynamic interfacial tensions of surfactant-containing solutions when necking is evident. The apparent interfacial tension obtained from a drop having a neck can be easily related to the actual interfacial tension if the drop neck diameter can be assumed to remain constant over a range of drop formation times. The model was tested by studying the dynamic interfacial tension of water drops growing in mineral oil with surfactant dissolved either in the water phase or the oil phase. For interfacial tensions exceeding 18 mN/m, neck formation was observed. Span 80, a nonionic surfactant, was found to provide data which agreed well with the model for concentrations below the cmc. Experimental data using the anionic surfactant SDS were found to provide reasonable agreement with the model only at low concentrations, when the build-up of interfacial charge is small.

For the study of surfactant adsorption kinetics, it was found that the DVT-10 tensiometer is a very convenient tool. Three surfactants were studied separately: SDS dissolved in the water phase, Span 80 dissolved in the oil phase, and Triton X-100 dissolved in the water phase. For all the surfactants studied, an increase in surfactant concentration or in drop formation time results in a decrease in the interfacial tension.

Three different adsorption models were tested for each surfactant. The anionic surfactant, SDS, was found to exhibit kinetic-controlled adsorption, likely due to an electrostatic potential barrier created at the interface by the adsorbed surfactant ions. Adsorption rates calculated with Equation [6.3] appeared to be independent of the surfactant concentration.

Span 80 was found to fit the short-time approximation of diffusion-controlled adsorption at concentrations below the cmc. Diffusion coefficients were calculated by using Equation [2.10]. Triton X-100 was found to exhibit diffusion-controlled adsorption as well, but the long-time approximation was required. The diffusion coefficients for Triton X-100 at concentrations below the cmc were calculated by using Equation [2.13]. For both Triton X-100 and Span 80 surfactants, the diffusion coefficients decreased with increasing surfactant concentration, likely due to micelle formation.

In order to determine the general applicability of short and long time diffusion approximations, the concept of a dimensionless parameter relating adsorption time, t_a, to a characteristic diffusion time, τ_D, was introduced. In the case of Triton X-100, the long time approximation was valid, and the ratio of t_a/τ_D was found to be much greater than one for all concentrations and drop formation times tested. In the case of Span 80, the short time approximation provided a good fit to the experimental data, and the ratio of t_a/τ_D was found to be on the order of unity or less for all concentrations and drop formation times tested.

A consideration of experimental data found in the literature for other surfactants led to the general conclusion that the ratio t_a/τ_D is useful in characterizing diffusion-controlled adsorption of surfactants. For values on the order of unity or less, the short diffusion time approximation, Equation [2.10], is valid. For values of t_a/τ_D that are much greater than unity, the long diffusion time approximation, Equation [2.13], is valid. In calculating τ_D,

approximate values of diffusion coefficient are acceptable, but great care must be taken to select an appropriate surface equation of state in order to avoid introducing large errors into the calculations.

This research work represents a first step in characterizing surfactant adsorption at the liquid-liquid interface using a drop volume tensiometer. Much work is still required in the area. Some recommendations for future research are elaborated below.

Synthetic surfactants may be toxic to soil micro-organisms. There is consequently much current interest in the use of biological surfactants. These biosurfactants must thus be characterized at the water / HOC interface. Research work should also focus on other type of HOC, with emphasis on halogenated and aromatic hydrocarbons.

An important challenge will be the characterization of mixed surfactant systems. Mixture of surfactants are more likely to be encountered in soil remediation practice. Procedures and models need to be developed for their characterization. Another interesting field of study is the incorporation of micellar kinetics into adsorption models. This work could help elucidate the dynamics of *in-situ* solubilization and micro-emulsification processes.

References

Adamczyk, Z. 1987, "Nonequilibrium Surface Tension for Mixed Adsorption Kinetics", *J. Colloid Interface Sci.*, **120**, pp. 477-485.

Adamson, A. W. 1990, *Physical Chemistry of Surfaces*, 5th edition, John Wiley & Sons Inc., New York.

Adeel, Z. and Luthy, R. G. 1995, "Sorption and Transport Kinetics of a Nonionic Surfactant Through an Aquifer Sediment", *Environ. Sci. Technol.*, **29**, pp. 1032-1042.

Amante, J. C., Scamehorn, J. F. and Harwell, J. H. 1991, "Precipitation of Mixtures of Anionic and Cationic Surfactants: Effect of Surfactant Structure, Temperature, and pH", *J. Colloid Interface Sci.*, **144**, pp. 243-253.

Bonfillon, A., Sicoli, F. and Langevin, D. 1994, "Dynamic Surface Tension of Ionic Surfactant Solutions", *J. Colloid Interface Sci.*, **168**, pp. 497-504.

Campanelli, J. R. and Wang, X. 1997A, "Effect of Neck Formation on the Measurement of Dynamic Interfacial Tension in a Drop Volume Tensiometer", *J. Colloid Interface Sci.*, **190**, in press.

Campanelli, J. R. and Wang, X. 1997B, "Comments on Modeling the Diffusion-controlled Adsorption of Surfactants", Submitted to *C. J. Ch. E.*

Dukhin, S. S., Krestzschmar, G. and Miller, R. 1995, *Dynamics of Adsorption at Liquid Interfaces*, Elsevier Science B. V., Amsterdam.

Forland, G. M., Samzeth, J., Hoiland, H. and Mortensen, K. 1994, "The Effect of Medium Chain Length Alcohols on the Micellar Properties of Sodium Dodecyl Sulfate in Sodium Chloride Solutions", *J. Colloid Interface Sci.*, **164**, pp. 163-167.

Fountain, J. C., Klimek, A. and Beikirch, M. G. 1991, *J. Harzard. Mater.,* **28**, pp. 295, in *Surfactant-Enhanced Subsurface Remediation*, ACS Symposium Series, **594**.

Fainerman, V. B. and Miller, R. 1995, "Dynamic Surface Tension Measurements in the Sub-Millisecond Range", *J. Colloid Interface Sci.*, **173**, pp. 245-254.

Gao, T. and Rosen, M. J. 1995, "Dynamic Surface Tension of Aqueous Surfactant Solutions: 7. Physical Significance of Dynamic Parameters and Induction Period", *J. Colloid Interface Sci.,* **172**, pp. 242-248.

Garandet, J. P., Vinet, B. and Gros, P. 1994, "Considerations on the Pendent Drop Method: A New Look at Tate's Law and Harkins' Correction Factor", *J. Colloid Interface Sci.,* **165**, pp. 351-354.

Hool, K. and Schuchardt, B. 1992, "A New Instrument for the Measurement of Liquid-Liquid Interfacial Tension and the Dynamics of Interfacial Tension Reduction", *Meas. Sci. Technol.*, 3, pp. 451-462.

Horozov, T. and Joos, P. 1995, "Dynamic Surface Tension of Surfactant Solutions Studied by Peaktensiometry", *J. Colloid Interface Sci.*, **173**, pp. 334-342.

Hua, X. Y., and Rosen, M. J. 1988, "Dynamic Surface Tension of Aqueous Surfactant Solutions 1. Basic Parameters", *J. Colloid Interface Sci.*, **124**, pp. 652-659.

Joos, P., Fang, J. P. and Serrien, G. 1992, "Comments on Some Dynamic Surface Tension Measurements by the Dynamic Bubble Pressure Method", *J. Colloid Interface Sci.*, **151**, pp. 144-149.

Joos, P. and Van Uffelen, M. 1995, "Theory on the Growing Drop Technique for Measuring Dynamic Interfacial Tension", *J. Colloid Interface Sci.*, **171**, pp. 297-305.

Kokal, S. L., Maini, B. B., and Woo, R. 1992, "Flow of Emulsions in Porous Media", in *Emulsions: Fundamentals and Applications in the Petroleum Industry*; Schramn, L. L. Ed., American Chemical Society, Washington, DC, pp. 219-262.

Liggieri, L., Ravera, F. and Passerone, A. 1995, "Dynamic Interfacial Tension Measurements by a Capillary Pressure Method", *J. Colloid Interface Sci.*, **169**, pp. 226-237.

Mackay, D. M. and Cherry, J. A. 1989, "Groundwater Contamination: Pump-and-treat Remediation", *Environ. Sci. Technol.*, **23**, pp. 630-641.

Myers, D. 1991, *Surfaces, Interfaces, and Colloids: Principles and Applications*, VCH Publishers, Inc., New York.

Miller, R., Joos, P. and Fainerman, V. B. 1994, "Dynamic Studies of Soluble Adsorption Layers", *Progr. Colloid Polymer Sci.*, **97**, pp. 188-193.

Miller, R. and Kretzschmar, G. 1991, "Adsorption Kinetics of Surfactants at Fluid Interfaces", *Adv. Colloid Interface Sci.*, **37**, pp. 97-121.

Molley, C., Touhami, Y. and Hornof, V.1996, "A Comparative Study of the Ready-made and in-Situ Formed Surfactants on the Interfacial Tension Measured by Drop Volume Tensiometry", *J. Colloid Interface Sci.*, **178**, pp. 523-529.

Nahringbauer, I. 1995, "Dynamic Surface Tension of Aqueous Polymer Solutions, 1: Ethyl(hydroxyethyl) cellulose (BERMOCOLL CST-103)", *J. Colloid Interface Sci.*, **176** pp. 318-328.

Nash, J. H. 1987, "Field Studies of In-situ Soil Washing", *U. S. Environmental Protection Agency, EPA/600/2-87/110,* Cincinnati, OH.

Okuda, I., Mcbride, J. F., Gleyzer, S. N. and Miller, C. T. 1996, "Physicochemical Transport Processes Affecting the Removal of Residual DNAPL by Nonionic Surfactant Solutions", *Environ. Sci. Technol.,* **30**, pp. 1852-1860.

Ouyang, Y., Mansell, R. S. and Rhue, R. D. 1995, "Emulsion-mediated Transport of Non-aqueous Phase Liquid in Porous Media: A Review", *Environ. Sci. Technol.*, **25**, pp. 269-290.

Pennell, K. D., Pope, G. A. and Abriola, L. M. 1996, "Influence of Viscous and Buoyancy Forces on the Mobilization of Residual Tetrachloroethylene during surfactant flushing", *Environ. Sci. Technol.,* **30**, pp. 1328-1335.

Pennell, K. D., Abriola, L. M. and Weber, Jr., W. J. 1993, "Surfactant-enhanced Solubilization of Residual Dodecane in Soil Column", *Environ. Sci. Technol.,* **27**, pp. 2332-2340.

Pierson, F. W. and Whitaker, S. 1976, "Studies of the Drop-Weight Method for Surfactant Solutions 1. Mathematical Analysis of the Adsorption of Surfactants at the Surface of a Growing Drop", *J. Colloid Interface Sci.,* **54**, pp. 203-209.

Ravera, F., Liggieri, L., Passerone, A. and Steinchen, A. 1994, "Sorption Kinetics at Liquid-Liquid Interfaces with the Surface-Active Component Soluble in Both Phases", *J. Colloid Interface Sci.*, **163**, pp. 309-314.

Ravera, F., Liggieri, L., Passerone, A. and Steinchen, A. 1993, "Sorption Kinetics Considered as a Renormalized Diffusion Process", *J. Colloid Interface Sci.*, **156**, pp. 109-116.

Rillaerts, E. and Joos, P. 1982, "Rate of Demicellization from the Dynamic Surface Tensions of Micellar Solutions", *J. Phys. Chem.*, **86**, pp. 3471-3478.

Rosen, M. J. and Song, L. D. 1996, "Dynamic Surface Tension of Aqueous Surfactant Solutions - 8. Effect of Spacer on Dynamic Properties of Gemini Surfactant Solutions", *J. Colloid Interface Sci.*, **179**, pp. 261-268.

Rosen, M. J. and Gao, T. 1995, "Dynamic Surface Tension of Aqueous Surfactant Solutions 5. Mixtures of Different Charge Type Surfactants", *J. Colloid Interface Sci.*, **173**, pp. 42-48.

Sabatini, D. A., Knox, R. C. and Harwell, J. H. 1995, *Surfactant-Enhanced Subsurface Remediation*, ACS Symposium Series, 594, American Chemical Society, New York.

Span 80 Product Information Bulletin, ICI Surfactants, Wilmington, DE (1996).

Tamura, T., Kaneko, Y., and Ohyama, M. 1995, "Dynamic Surface Tension and Foaming Properties of Aqueous Polyoxyethylene N-Dodecyl Ether Solutions", *J. Colloid Interface Sci.,* **173**, pp. 493-499.

Touhami, Y., Hornof, V. and Neale, G. H. 1994, "Interfacial Tension Behavior of an Acidified Oil / Surfactant System", *J. Colloid Interface Sci.,* **166**, pp. 506-508.

Van Hunsel, J., Bleys, G. and Joos, P. 1986, "Adsorption Kinetics at the Oil / Water Interface", *J. Colloid Interface Sci.*, **114**, pp. 432-441.

Van Uffelen, M. and Joos, P. 1994, in "Dynamic Surface Tension of Surfactant Solutions Studied by Peaktensiometry", *J. Colloids Interface Sci.*, **173**, pp. 334-342.

Wang, X. and Campanelli, J. 1997, "Dynamic Interfacial Tension and Surfactant Adsorption Rate", Proceeding of the *25th CSCE Annual conference*, Vol. 5, Sherbrooke, pp. 103-112.

Ward, A. F. H. and Tordai, L. 1946, "Time-Dependence of Boundary Tensions of Solutions - I. The Role of Diffusion in Time-Effect ", *J. Chem. Physics*, **14**, pp. 453-459.

Weber, W. J. J_R. and Digiano, F. A. 1996, *Process Dynamics in Environmental Systems*, John Wiley & Sons, Inc., New York.

Wilke, C. R. and Chang, P. 1955, "Correlation of diffusion coefficients in dilute solutions", *A.I.Ch.E. Journal*, **1**, pp. 264.

Wilkinson, M. C. 1972, "Extended Use of, and Comments on, the Drop Weight (Drop Volume) Technique for the Determination of Surface and Interfacial Tension", *J. Colloid Interface Sci.*, **40**, pp. 14-23.

Wilson, J. L., Conrad, S. H., Mason, W. R., Peplinski, W. and Hagan, E. 1990, "Laboratory Investigations of Residual Liquid Organics from Spills, Leaks and Disposal of Hazardous Wastes in Groundwater", *U.S. EPA, EPA/600/6-90/004,* Ada, OK.

Xu, Y.1995, "Dynamic Interfacial Tension Between Bitumen and Aqueous Sodium Hydroxide Solutions", *Energy & Fuels*, **9**, pp. 148-154.

Glossary

ROMAN LETTERS

a_L Langmuir constant in Equation [5.13], mol/m^3

b radius of curvature at the bottom of the suspended drop, m

c surfactant concentration in the subsurface, mol/m^3

C_o surfactant concentration in the bulk, mol/m^3

ΔC_s equal to C_0-C, mol/m^3

d capillary diameter, m

d_n the neck diameter at the moment of detachment, m

d_p diameter of a particle of the porous media, m

D diffusion coefficient, m^2/s

k_{ad} adsorption rate constant, m/s

k_{des} desorption rate constant, 1/s

k_h constant term related to hydrostatic pressure, Pa

N_{ca} capillary number, dimensionless

N_B bond number, dimensionless

p perimeter, m

P_n net pressure acting on the neck at the moment of detachment, Pa

P_h hydrostatic pressure, Pa

ΔP excess pressure, Pa

q	Darcy velocity, m/s
r	drop radius, m
r_d	capillary tip radius, m
r_n	pendant drop radius at the neck, m
R	gas law constant in equation [2.3], 8.314 g $cm^2/(s^2 mol\ K)$
t	drop formation time, s
t_a	adsorption time, defined in Equation [2.4] for a growing drop, s
T	absolute temperature, K
ν	solute molar volume in equation [6.4], m^3/mol
V	drop volume at detachment, m^3
V_n	the volume of the drop including the neck, m^3
w	drop weight, N
z_0	height of the pendant drop, m

GREEK LETTERS

γ	interfacial tension, N/m
γ_{app}	apparent interfacial tension, N/m
γ_e	equilibrium interfacial tension, N/m
γ_o	interfacial tension of the pure interface, N/m
γ_{ow}	interfacial tension between the organic and aqueous phases, N/m
Γ	interfacial concentration of surfactant, mol/m^2
Γ_e	equilibrium interfacial concentration of surfactant, mol/m^2
Γ_∞	maximum interfacial concentration of surfactant, mol/m^2
λ	dummy variable in Equation [2.5], dimensionless
ϱ_H	density of the heavy phase, kg/m^3
ϱ_L	density of the light phase, kg/m^3
$\Delta\varrho$	difference in fluid densities, kg/m^3
τ_D	characteristic surfactant diffusion time, defined in Equation [2.15], s
μ_w	viscosity of water, Pa.s
μ	viscosity of the solution, Pa.s